

The two-body reduced density matrix of the high-density electron gas

P. ZIESCHE

Max-Planck-Institut für Physik komplexer Systeme
Nöthnitzer Str. 38, D-01187 Dresden, Germany, pz@pks.mpg.de

PACS 71.10.Ca, 05.30.Fk

(Dated: draft of November 2, 2018)

For the first time, the *cumulant* 2-body reduced density matrix (= 2-matrix) of the spin-unpolarized homogeneous electron gas (HEG) is considered. This γ_c proves to be the common source for both the momentum distribution $n(k)$ and the static structure factor $S(q)$. Within many-body perturbation theory, this γ_c is given by only *linked* diagrams (with 2 open particle-hole lines as well as with closed loops and interaction lines). Here it is worked out in detail, how the 1-body quantity $n(k)$ follows from the 2-body quantity γ_c - through a certain contraction procedure, cf Eqs.(2.25)-(2.28). In particular, this γ_c is developed for the high-density HEG. Its correctness is checked by deriving from it $n(k)$ and $S(q)$, known from the random-phase approximation (RPA). This study opens the way to a more sophisticated HEG description in terms of cumulant geminals or/and variational methods. Besides, the cumulant structure factor (CSF) of the exchange in lowest order is explicitly given and sum rules for the CSFs and their small- and large- q behavior (beyond RPA) are systematically summarized within the plasmon sum rule, coalescing theorems, and the inflexion-point trajectory.

List of Symbols/Shorthands/Abbreviations

RDM reduced density matrix, SR sum rule, ρ homogeneous electron density

MD momentum distribution $n(k)$, $f(r)$ 1-body RDM

PD pair density $g(r)$, CPD cumulant PD $h(r)$: $g(r) = 1 - \frac{1}{2}f^2(r) - h(r)$

SF structure factor $S(q)$, CSF cumulant SF $C(q)$: $S(q) = 1 - \frac{1}{2}F(q) - C(q)$

"a" antiparallel spin: $g_a(r) \leftrightarrow S_a(q)$, $h_a(r) \leftrightarrow C_a(q)$

"p" parallel spin: $g_p(r) \leftrightarrow S_p(q)$, $h_p(r) \leftrightarrow C_p(q)$

FT Fourier transform, $F(q) = \text{FT of } f^2(r)$, FS Fermi surface $|\mathbf{k}| = 1$

I. INTRODUCTION

The lowest-level quantum-kinematics of an extended many-electron system (within the Born-Oppenheimer approximation) is contained in 1- and 2-body densities and reduced density matrices (RDMs): $\rho_1(1)$ = electron density, $\gamma_1(1|1')$ = 1-body RDM (1-matrix), $\rho_2(1, 2)$ = pair density (PD), $\gamma_2(1|1', 2|2')$ = 2-matrix. The well-trying and widely used density functional theory (DFT) yields ρ_1 (but not γ_1 and ρ_2). If a density-matrix functional theory would exist, it would yield γ_1 (but not ρ_2); if a pair-density functional theory would exist, it would yield ρ_2 (but not γ_1). If an effective 2-body scheme would exist, which yields approximately the 2-matrix γ_2 , then from it would follow both the PD ρ_2 (by taking the diagonal elements) and the 1-matrix γ_1 (by means of the contraction procedure $2' = 2$ and $\int d2 \gamma_2(1|1', 2|2)$). For extended systems this requires the cumulant decomposition of γ_2 . In this paper (it continues from [5, 42, 53] and is related to [36, 38]), the **cumulant 2-matrix** γ_c (dimensionless: χ) is developed as a decisive key quantity and its properties are studied for a "simple" model system, namely the high-density spin-unpolarized homogeneous electron gas (HEG).

Although not present in the Periodic Table, this HEG is still an important and so far unsolved model system for the electronic structure theory, cf e.g. [1]. Its advantage: pure "correlation" and no "multiple-scattering". In its spin-unpolarized version, the HEG ground state (GS) is characterized by only one parameter r_s , such that a sphere with this **Wigner-Seitz radius** r_s contains *on average* one electron [2]. It determines the Fermi wave number as $k_F = 1/(\alpha r_s)$ in atomic units (a.u.) with $\alpha = [4/(9\pi)]^{1/3} \approx 0.521062$ and it measures simultaneously both the interaction strength and the homogeneous electron density ρ , such that high density corresponds to weak interaction and hence weak correlation [3]. For recent papers on this limit cf [4–12]. $r_s = 0$ corresponds to the ideal Fermi gas. Its GS energy per particle is $e_0 = 3/10$, measured in units of k_F^2 . The Coulomb repulsion $v(q) = q_c^2/q^2$ with $q_c^2 = 4\alpha r_s/\pi$ causes deviations. This is in lowest order the exchange energy $e_x = -(3/4\pi)\alpha r_s$. But in next order the long range of the Coulomb repulsion makes the correlation energy e_{corr} , defined by $e = e_0 + e_x + e_{\text{corr}} + O(r_s)$, to behave non-analytically at the high-density limit: $e_{\text{corr}} \sim r_s^2[\ln r_s + \text{const} + O(r_s)]$ [13–15, 38]. This non-analytical behavior of e carries over to the kinetic and potential components, t respectively v , through the virial theorem after

March (1958)[16]:

$$v = r_s \frac{d}{dr_s} e, \quad t = -r_s^2 \frac{d}{dr_s} \frac{1}{r_s} e. \quad (1.1)$$

The energy components t and v follow from the simplest quantum-kinematical quantities, namely $n(k)$ and $S(q)$, the momentum distribution (MD) and the (static) structure factor (SF), respectively:

$$t = \int_0^\infty d(k^3) n(k) \frac{k^2}{2}, \quad \int_0^\infty d(k^3) n(k) = 1, \quad \int_0^\infty d(k^3) n(k)[1 - n(k)] = c, \quad (1.2)$$

$$v = - \int_0^\infty \frac{d(q^3)}{3 \cdot 4} [1 - S(q)] \frac{q_c^2}{q^2}, \quad S(0) = 0, \quad \int_0^\infty d(q^3) [1 - S(q)] = 1 + c_1. \quad (1.3)$$

k and q are measured in units of k_F and r in units of k_F^{-1} . The quantity c is hereforth referred to as Löwdin parameter, because Löwdin was the first one who queried the meaning of the trace of the squared 1-matrix. Because of $0 \leq n(k) \leq 1$, c measures the r_s -dependent non-idempotency of $n(k)$, being zero for $r_s = 0$ (ideal Fermi gas) and increasing with r_s . Thus c measures simultaneously the strength of correlation. Note its particle-hole symmetry. c_1 is another (short-range) correlation parameter, also vanishing for $r_s \rightarrow 0$.

Describing **electron pairs**, one has to distinguish SFs $S_{a,p}(q)$ for pairs with antiparallel spin ("a") and with parallel spins ("p") and corresponding pair densities (PDs) $g_{a,p}(r)$, where $g_a(r)$ and $g_p(r)$ describe the Coulomb hole and the Fermi hole, respectively. The $g_{a,p}(r)$ and $S_{a,p}(q)$ are mutually related through Fourier transform (FT):

$$g_a(r) - 1 = \int_0^\infty d(q^3) \frac{\sin qr}{qr} S_a(q) \quad \leftrightarrow \quad S_a(q) = \alpha^3 \int_0^\infty d(r^3) \frac{\sin qr}{qr} \frac{1}{2} [g_a(r) - 1], \quad (1.4)$$

$$g_p(r) - 1 = \int_0^\infty d(q^3) \frac{\sin qr}{qr} [S_p(q) - 1] \quad \leftrightarrow \quad S_p(q) - 1 = \alpha^3 \int_0^\infty d(r^3) \frac{\sin qr}{qr} \frac{1}{2} [g_p(r) - 1].$$

From this follow the "total" PD $g(r) = [g_a(r) + g_p(r)]/2$ and the "total" SF $S(q) = S_a(q) + S_p(q)$:

$$g(r) - 1 = \int_0^\infty d(q^3) \frac{\sin qr}{qr} \frac{1}{2} [S(q) - 1] \quad \leftrightarrow \quad S(q) - 1 = \alpha^3 \int_0^\infty d(r^3) \frac{\sin qr}{qr} [g(r) - 1]. \quad (1.5)$$

$S_{a,p}(0) = 0$ fix the normalizations of $1 - g_{a,p}(r)$, known as the perfect screening SR, whereas the coalescing (or on-top) values $g_a(0)$ and $g_p(0) = 0$ fix the normalizations of $S_a(q)$ and

$S_p(q) - 1$, respectively. $g_a(0) = 1 - c_1$ or $g(0) = (1 - c_1)/2$ shows the physical meaning of c_1 . It determines the short-range correlation in terms of $g_a(0)$, the on-top value of the Coulomb hole $g_a(r)$ with $0 \leq g_a(0) \leq 1$. For further details (normalizations) cf (B.1), (B.2).

In view of Eqs.(1.2) and (1.3), one may ask which peculiarities of $n(k)$ and $S_{a,p}(q)$ cause the non-analyticities of t and v , respectively. As shown in [6], the above-mentioned drastic changes, when switching on the long-range Coulomb interaction, show up in the redistribution of the non-interacting MD $n_0(k) = \Theta(1 - k)$ within thin layers (thickness q_c) inside and outside the Fermi surface $|\mathbf{k}| = 1$ and with a remaining finite jump discontinuity at $|\mathbf{k}| = 1$: $z_F = n(1^-) - n(1^+)$, $0 \leq z_F \leq 1$. They show up also in the behavior of $S(q)$ within a small spherical region (radius q_c) around the origin of the reciprocal space with the plasmon SR $S(q \ll q_c) = q^2/(2\omega_{pl}) + \dots$ [17, 18], which causes an inflexion point $q_{\text{infl}}, S_{\text{infl}} \sim \omega_{pl}$, where $\omega_{pl} = q_c/\sqrt{3}$ is the plasma frequency, measured in units of k_F^2 . The mentioned non-analyticities and redistributions let ordinary perturbation theory fail, e.g. with $S(q \rightarrow 0) \sim 1/q$ and $n(k) = n_0(k) + \Delta n(k)$ with $n_0(k) = \Theta(1 - k)$ and $\Delta n(k \rightarrow 1^\pm) \sim \pm 1/(k - 1)^2$. That the GS energy $e(r_s)$ diverges in 2nd order, has been shown by Heisenberg (1947) [13]. Macke (1950) [14] has repaired this failure by means of an appropriate, physically plausible **partial summation of higher-order perturbation terms** for the GS energy per particle $e(r_s)$, a way which has been developed further by Gell-Mann and Brueckner (1957) [15]. This so-called ring-diagram summation, cf Fig.1, is also known as the random phase approximation (RPA). This summation has been developed for $n(k)$ by Daniel/Vosko (1960) [19] and Kulik (1961) [20], an analytical extrapolation for $n(k)$ is given in [21, 22], for the spin-polarized case see [23], recent quantum Monte Carlo calculations of $n(k)$ for $r_s = 1, \dots, 10$ are in [24], z_F for high-densities is in [25], z_F calculated for $r_s < 55$ is in [26]. The ring-diagram summation for $S(q)$ has been done by Glick/Ferrell (1960) [27], Geldart (1967) [28], and Kimball (1976) [29]. For attempts to go beyond RPA cf eg [24, 30]. The on-top behavior of $g_{a,p}$ (describing the short-range correlation) influence the large- q behavior of $S_{a,p}(q)$ and $n(k)$. This comes from theorems referred here as the coalescing cusp and curvature theorems, cf [31] and [32] and App.B.

With $n(k)$ also t is available (but not v) and with $S(q)$ it is available v (but not t). Does a quantity exist which contains both $n(k)$ and $S(q)$? "Old" and recent attempts in that

direction (with variational or direct calculations of the 2-matrix) are in [59, 65, 66]. In [12] it has been shown that the self-energy $\Sigma(k, \omega)$ as a *functional* of $t(\mathbf{k}) = k^2/2$ and $v(\mathbf{q}) = q_c^2/q^2$ is such a quantity [69]. Here it is shown - using the concept of reduced density matrices (RDMs) - that $n(k)$ and $S(q)$ have their common origin in a quantity called 'cumulant 2-matrix', $\chi(1|1', 2|2')$ with the symbolic variable $1 = (\mathbf{r}_1, \sigma_1)$. This matrix appears if one tries to represent the 2-matrix of an interacting system in terms of the 1-matrix (according to an independent-particle or Hartree-Fock model). There remains an irreducible part, which can not be reduced due to correlation. For the PD and for the SF, these **cumulant decompositions** are

$$g_a(r) = 1 - h_a(r) , \quad S_a(q) = -C_a(q) , \quad (1.6)$$

$$g_p(r) = 1 - f^2(r) - h_p(r) , \quad S_p(q) = 1 - \frac{1}{2}F(q) - C_p(q) . \quad (1.7)$$

Note the asymmetry with respect to "a" (Coulomb hole) and "p" (Fermi hole). With the "total" cumulants $h(r) = [h_a(r) + h_p(r)]/2$ and $C(q) = C_a(q) + C_p(q)$ it follows

$$g(r) = 1 - \frac{1}{2}f^2(r) - h(r) , \quad S(q) = 1 - \frac{1}{2}F(q) - C(q) . \quad (1.8)$$

$f(r)$ is the dimensionless 1-matrix [following from $n(k)$, cf (2.4)] and $F(q)$ - referred to as HF-function - is the FT of $f^2(r)$, cf (B.15). $h_{a,p}(r)$ are the cumulant PDs (CPDs) and their FTs are the cumulant SFs (CSFs) $C_{a,p}(q)$:

$$h_a(r) = \int_0^\infty d(q^3) \frac{\sin qr}{qr} C_a(q) \quad \leftrightarrow \quad C_a(q) = \alpha^3 \int_0^\infty d(r^3) \frac{\sin qr}{qr} \frac{1}{2} h_a(r) , \quad (1.9)$$

$$h_p(r) = \int_0^\infty d(q^3) \frac{\sin qr}{qr} C_p(q) \quad \leftrightarrow \quad C_p(q) = \alpha^3 \int_0^\infty d(r^3) \frac{\sin qr}{qr} \frac{1}{2} h_p(r) . \quad (1.10)$$

Within RDM theory one can show that the cumulant 2-matrix $\chi(1|1', 2|2')$ is the source for: (i) the CSF $C(q)$ [or equivalently the CPD $h(r)$] and (ii) also for the MD $n(k)$. Whereas (i) results simply from $\chi(1|1, 2|2)$, i.e. taking the diagonal elements $1' = 1, 2' = 2$, the case (ii) follows from the slightly more complicated RDM contraction of $\chi(1|1', 2|2')$ with $2' = 2$, $\int d2 \chi(1|1', 2|2)$ and FT. The Eqs.(1.9) and (1.10) contain the CSF properties (B.1) and (B.2) needed below.

General remarks on **RDMs and cumulants**: Whereas finite many-body systems can be described by many-body wave functions $\Phi(1,2,\dots)$ as solutions of a Schrödinger equation, extended systems have to be described by a hierarchy of N -representable RDMs as solutions of the BBGKY-like hierarchy of contracted Schrödinger equations. And: whereas for finite systems the concept of cumulant (2-body, 3-body, ...) matrices *can* be applied, for extended systems it is a *must*, because - unlike the RDMs - all these cumulant matrices are *size-extensive* entities, what allows the thermodynamic limit with $N \rightarrow \infty$, $\Omega \rightarrow \infty$, $\rho = N/\Omega = \text{const}$. Closely related with this property is that they are given within perturbation theory by non-vacuum *linked* Feynman diagrams. In App.A, the systematic definition of cumulant matrices in terms of generating functionals is summarized. Recent (quantum chemical) papers on RDMs, cumulants, contracted Schrödinger equations, correlation strength, correlation entropy, quantum entanglement, Berry phases etc. are [55]-[64] and refs. therein. [65] and [66] deal (for finite systems) with variational calculations of the 2-matrix. Recent HEG papers are [67] and [68] and refs. within.

Here is roughly sketched, what will be presented in Secs. II, III, IV in more detail. In this paper it is aimed to present χ in the RPA with all those terms of χ contributing to the correlation energy e_{corr} terms up to $r_s^2 \ln r_s$ and r_s^2 . The correctness of this χ is controlled/checked by deriving $n(k)$ and $S(q)$. A comparison is performed between these 'new' RPA results with the 'old' ones of Daniel/Vosko [19], Kulik [20], and Kimball [29], respectively. For this purpose the diagrams of Figs.1-5 are needed. Fig.1 shows the Yukawa-like screening of the bare (long-range) Coulomb repulsion $v(q) = q_c^2/q^2$, replacing it by the frequency-dependent interaction $v(q, \eta) = v(q)/[1 + v(q)Q(q, \eta)]$, where $Q(q, \eta)$ is the particle-hole propagator (C.3). The bare Coulomb repulsion shows up in divergencies: for the correlation energy e_{corr} see [13], for $n(k)$ and $S(q)$ see [6]. These divergencies are eliminated through Macke's partial summation of diagrams. Fig.2a shows the interaction of 2 particle-hole lines running from $1'$ to 1 and from $2'$ to 2. This is called "d" = direct diagram to distinguish it from "x" = exchange diagram of Fig.3a with one line running from $1'$ to 2 and another one from $2'$ to 1. These lowest-order RPA terms of Figs. 2a and 3a are called χ_{dr} and χ_{xr} , respectively, "r" = ring-diagram summation of Fig. 1. The cumulant matrices $\chi_{\text{dr,xr}}$ yield the CPDs $h_{\text{dr,xr}}$ and the CSFs $C_{\text{dr,xr}}$ of Figs. 2b and 3b and the interaction energies of Figs. 2c and 3c. But how to obtain $\Delta n(k)$? Using the self-energy

$\Sigma(k, \omega)$, the lowest-order Σ - diagrams are in Figs.4c and 5c: $\Delta n(k) = n_r(k) + n_x(k) + \dots$. Of course, RDM-theory must end up with the same results. Indeed, $n_r(k)$ of Fig.4c comes from χ_{xr} of Fig.3a by the contraction $2' = 2$ and $\int d2$, indicated in Fig.4b by a small circle with the final result $n_r(k)$ of Fig.4c. Similarly, $n_x(k)$ of Fig.5c comes from the ladder diagram (in its exchange version) of Fig.5a, contraction makes Fig.5b with the final result $n_x(k)$ of Fig.5c. Contraction in terms of diagrams mean to transform a 2-line diagram into a 1-line-diagram. This study opens the door for variational 2-matrix calculations and for discussing HEG in terms of cumulant geminals and their weights.

The outline of the paper is as follows. In Sec.II the basic definitions of RDMs, their cumulant decompositions and the contraction SR are presented. It is derived in detail how the 2-body quantities $S(q)$ and $g(r)$ with its cumulant pedants $C(q)$ and $h(r)$, together with the 1-body quantity $n(k)$, follow from the cumulant 2-body matrix χ . The decisive contraction procedure is in Eqs.(2.25)-(2.28). In Secs.III and IV the lowest-order cumulant 2-matrices and what follows from them are presented. Sec.V gives a summary and an outlook. App.A explains the exponential-linked-diagram theorem as the base for a systematic cumulant decompositions. App.B deals with SF properties in terms of the coalescing cusp and curvature theorems, of the plasmon SR, and of the inflexion-point trajectory. Table 1 and 2 contain the small- and large q -behavior of the CSFs and SFs (similar as in [36]). In App.C the particle-hole propagator, the Macke function $I(q)$ and contour integrations are described. App.D lists characteristic correlation parameters, vanishing for $r_s \rightarrow 0$.

II. BASIC DEFINITIONS AND RELATIONS

2.1 The 1-matrix and the 2-matrix: definitions and properties

The starting point is the definition of the 1-matrix γ_1 and of the 2-matrix γ_2 for the HEG-GS in terms of creation and annihilation operators, ψ_1^\dagger and ψ_1 , respectively:

$$\gamma_1(1|1') = \langle \psi_1^\dagger, \psi_1 \rangle, \quad \gamma_2(1|1', 2|2') = \langle \psi_1^\dagger, \psi_2^\dagger, \psi_2, \psi_1 \rangle. \quad (2.1)$$

The shorthands $1 = (\mathbf{r}_1, \sigma_1)$ and $\int d1 = \sum_{\sigma_1} \int d^3r_1$ are used. The hermiticity is obvious and Fermi symmetry means $\gamma_2 \rightarrow -\gamma_2$ if 1 and 2 or 1' and 2' are interchanged. $\hat{N} = \int d1 \psi_1^\dagger \psi_1$

is the total particle-number operator. The bra vector " \langle " as well as the ket vector " \rangle " are N -body states, therefore $|\psi_1\rangle$ and $\langle\psi_1^\dagger$ are $(N-1)$ -body states, thus

$$\int d1 \langle\psi_1^\dagger\psi_1\rangle = N, \quad \int d1d2 \langle\psi_1^\dagger\psi_2^\dagger\psi_2\psi_1\rangle = N(N-1) \quad (2.2)$$

holds for the normalization. The contraction SR

$$\int d2 \langle\psi_1^\dagger\psi_2^\dagger\psi_2\psi_1\rangle = \gamma_1(1|1')(N-1) \quad (2.3)$$

describes how the 1-matrix γ_1 for finite N results from the 2-matrix γ_2 .

It follows the spin structure of γ_1 , the dimensionless 1-matrix $f(r)$ and its FT:

$$\begin{aligned} \gamma_1(1|1') &= \frac{1}{2}\delta_{\sigma_1,\sigma_1'}\gamma_1(\mathbf{r}_1|\mathbf{r}_1'), \quad \gamma_1(\mathbf{r}_1|\mathbf{r}_1') = \rho f(r_{11'}), \quad r_{11'} = |\mathbf{r}_1 - \mathbf{r}_1'|, \\ f(r) &= \int_0^\infty d(k^3) \frac{\sin kr}{kr} n(k), \quad f(0) = \int_0^\infty d(k^3) n(k) = 1, \end{aligned} \quad (2.4)$$

$f'(0) = 0$, $f''(0) = -2t/3$ (with $t_0 = 3/10$ and $f_0''(0) = -1/5$ for $r_s = 0$). Its natural orbitals are plane waves, because the system is extended and homogeneous. $n(k)$ is the momentum distribution (MD), \mathbf{k} and \mathbf{r} are measured in units of k_F and k_F^{-1} , respectively.

The symmetric and antisymmetric 2-body spin functions

$$\delta_\pm(\sigma_1|\sigma_1', \sigma_2|\sigma_2') = \frac{1}{2}(\delta_{\sigma_1,\sigma_1'}\delta_{\sigma_2,\sigma_2'} \pm \delta_{\sigma_1,\sigma_2'}\delta_{\sigma_2,\sigma_1'}) \quad \text{with} \quad \frac{1}{4} \sum_{\sigma_{1,2}} \delta_\pm(\sigma_1|\sigma_1, \sigma_2|\sigma_2) = \begin{cases} 3/4 \\ 1/4 \end{cases} \quad (2.5)$$

enter the spin structure of $\gamma_2(1|1', 2|2')$ as

$$\gamma_2(1|1', 2|2') = \delta_-(\sigma_1|\sigma_1', \sigma_2|\sigma_2') \gamma_2^+(\mathbf{r}_1|\mathbf{r}_1', \mathbf{r}_2|\mathbf{r}_2') + \delta_+(\sigma_1|\sigma_1', \sigma_2|\sigma_2') \gamma_2^-(\mathbf{r}_1|\mathbf{r}_1', \mathbf{r}_2|\mathbf{r}_2') \quad (2.6)$$

[23, 34]. It defines - together with the basic definition (2.1) - the singlet 2-matrix γ_2^+ and the triplet 2-matrix γ_2^- , being (in space) symmetric and antisymmetric for the interchanges $\mathbf{r}_1 \leftrightarrow \mathbf{r}_2$ or $\mathbf{r}_1' \leftrightarrow \mathbf{r}_2'$, respectively. The normalizations

$$\int d^3r_1 d^3r_2 \gamma_2^\pm(\mathbf{r}_1|\mathbf{r}_1, \mathbf{r}_2|\mathbf{r}_2) = \frac{N}{2} \left(\frac{N}{2} \pm 1 \right) \quad (2.7)$$

follow from the contractions

$$\int d^3r_2 \gamma_2^\pm(\mathbf{r}_1|\mathbf{r}_1', \mathbf{r}_2|\mathbf{r}_2) = \frac{1}{2} \gamma_1(\mathbf{r}_1|\mathbf{r}_1') \left(\frac{N}{2} \pm 1 \right), \quad (2.8)$$

which are in their turn consequences of the total normalization (2.2) and the singlet-triplet representation (2.6). Eqs.(2.7) and (2.8) show the necessity to find an equivalent writing for γ_2 , which allows the thermodynamic limit with $N \rightarrow \infty$, $\Omega \rightarrow \infty$, $\rho = N/\Omega = \text{const.}$ This is just done by means of an additive decomposition of γ_2 in a Hartee-Fock like term γ_{HF} , which is defined in terms of the (full, exact) 1-matrix γ_1 only, and a non-reducible remainder - the cumulant 2-matrix γ_c . Thus $\gamma_2 = \gamma_{\text{HF}} - \gamma_c$ as the first step of a more general expansion, see App.A.

2.2 The HF approximation

The 2-matrix in a Hartree-Fock like approximation (in terms of the exact 1-matrix only) is

$$\gamma_{\text{HF}}(1|1', 2|2') = \gamma_1(1|1')\gamma_1(2|2') - \gamma_1(1|2')\gamma_1(2|1') . \quad (2.9)$$

This may be also addressed "exact exchange". Using Eq.(2.4), the same structure (2.6) as for the total 2-matrix $\gamma_2(1|1', 2|2')$ results:

$$\gamma_{\text{HF}}(1|1', 2|2') = \delta_-(\sigma_1|\sigma'_1, \sigma_2|\sigma'_2)\gamma_{\text{HF}}^+(\mathbf{r}_1|\mathbf{r}'_1, \mathbf{r}_2|\mathbf{r}'_2) + \delta_+(\sigma_1|\sigma'_1, \sigma_2|\sigma'_2)\gamma_{\text{HF}}^-(\mathbf{r}_1|\mathbf{r}'_1, \mathbf{r}_2|\mathbf{r}'_2) \quad (2.10)$$

with

$$\begin{aligned} \gamma_{\text{HF}}^\pm(\mathbf{r}_1|\mathbf{r}'_1, \mathbf{r}_2|\mathbf{r}'_2) &= \gamma_1(\mathbf{r}_1|\mathbf{r}'_1)\gamma_1(\mathbf{r}_2|\mathbf{r}'_2) \pm \gamma_1(\mathbf{r}_1|\mathbf{r}'_2)\gamma_1(\mathbf{r}_2|\mathbf{r}'_1) \\ &= \frac{\rho^2}{4} [f(r_{11'})f(r_{22'}) \pm f(r_{12'})f(r_{21'})] . \end{aligned} \quad (2.11)$$

Their normalizations

$$\int d^3r_1 d^3r_2 \gamma_{\text{HF}}^\pm(\mathbf{r}_1|\mathbf{r}_1, \mathbf{r}_2|\mathbf{r}_2) = \frac{N}{2} \left(\frac{N}{2} \pm 1 \right) \mp \frac{N}{2} c \quad (2.12)$$

contain the above introduced Löwdin parameter c , which is originally defined by

$$1 - c = \frac{2}{N} \int d^3r_1 d^3r_2 \frac{1}{4} |\gamma_1(\mathbf{r}_1|\mathbf{r}_2)|^2 = \alpha^3 \int_0^\infty d(r_{12}^3) \frac{1}{2} f^2(r_{12}) = \int_0^\infty d(k^3) n^2(k) . \quad (2.13)$$

Note $\rho \int d^3r_1 = \rho\Omega = N$ and note that the homogeneous density ρ , measured in units of k_{F}^3 , equals $1/(3\pi^2)$ and that $d^3r_{12}/(3\pi^2) = \alpha^3 d(r_{12}^3)$, $\alpha = [4/(9\pi)]^{1/3}$.

The contractions of γ_{HF}^\pm are

$$\int d^3r_2 \gamma_{\text{HF}}^\pm(\mathbf{r}_1|\mathbf{r}'_1, \mathbf{r}_2|\mathbf{r}_2) = \frac{1}{2}\gamma_1(\mathbf{r}_1|\mathbf{r}'_1) \left(\frac{N}{2} \pm 1 \right) \mp \frac{1}{2} c(\mathbf{r}_1|\mathbf{r}'_1) , \quad (2.14)$$

where

$$c(\mathbf{r}_1|\mathbf{r}'_1) = \rho \int \frac{d^3k}{4\pi/3} c(k) e^{i\mathbf{k}\mathbf{r}_{11'}} , \quad c(k) = n(k)[1 - n(k)] , \quad \int d^3r c(\mathbf{r}|\mathbf{r}) = Nc . \quad (2.15)$$

$c(k)$ and $c(\mathbf{r}, \mathbf{r}')$ are referred to as "Löwdin function" and "Löwdin matrix", respectively. $[c(k)$ appears in [62] as $-2e_k$].

2.3 The cumulant decomposition and cumulant geminals

With this prelude, the above mentioned decomposition

$$\gamma_2(1|1', 2|2') = \gamma_{\text{HF}}(1|1', 2|2') - \gamma_c(1|1', 2|2') \quad (2.16)$$

defines the cumulant 2-matrix γ_c . Its spin-structure is similar as in (2.6) and (2.10)

$$\gamma_c(1|1', 2|2') = \delta_-(\sigma_1|\sigma'_1, \sigma_2|\sigma'_2) \gamma_c^+(\mathbf{r}_1|\mathbf{r}'_1, \mathbf{r}_2|\mathbf{r}'_2) + \delta_+(\sigma_1|\sigma'_1, \sigma_2|\sigma'_2) \gamma_c^-(\mathbf{r}_1|\mathbf{r}'_1, \mathbf{r}_2|\mathbf{r}'_2) \quad (2.17)$$

and it defines (through $\gamma_2^\pm = \gamma_{\text{HF}}^\pm - \gamma_c^\pm$) the cumulant 2-matrices γ_c^\pm with the normalization

$$\int d^3r_1 d^3r_2 \gamma_c^\pm(\mathbf{r}_1|\mathbf{r}_1, \mathbf{r}_2|\mathbf{r}_2) = \mp \frac{N}{2} c , \quad (2.18)$$

following from the normalizations (2.7) and (2.12) . This ensures the normalization of γ_c to be $\int d1d2 \gamma_c(1|1, 2|2) = Nc$, as it should. With the help of Eqs.(2.8) and (2.14) the contractions of γ_c^\pm are

$$\int d^3r_2 \gamma_c^\pm(\mathbf{r}_1|\mathbf{r}'_1, \mathbf{r}_2|\mathbf{r}_2) = \mp \frac{1}{2} c(\mathbf{r}_1|\mathbf{r}'_1) . \quad (2.19)$$

Eqs.(2.18) and (2.19) show that the χ_c^\pm are size-extensively normalized and contracted. With $\gamma_c^\pm = \frac{\rho^2}{4} \chi_\pm$, the dimensionless cumulant 2-matrices χ_\pm are introduced. Their normalization follows from (2.18) as

$$\alpha^3 \int_0^\infty d(r_{12}^3) \chi_\pm(\mathbf{r}_1|\mathbf{r}_1, \mathbf{r}_2|\mathbf{r}_2) = \mp 2c . \quad (2.20)$$

The introduction of the singlet/triplet matrices γ_c^\pm and χ_\pm , is only a necessary intermediate step to present its spin-parallel/antiparallel components $\chi_{\text{p,a}}$ in terms of linked diagrams. For diagonal spins $\sigma'_{1,2} = \sigma_{1,2}$ it is $\delta_\pm(\sigma_1|\sigma_1, \sigma_2|\sigma_2) = (1 \pm \delta_{\sigma_1, \sigma_2})/2$. So for antiparallel spins ($\sigma_1 = -\sigma_2$, hence $\delta_{\sigma_1, \sigma_2} = 0$), respectively parallel spins ($\sigma_1 = \sigma_2$, hence $\delta_{\sigma_1, \sigma_2} = 1$) the spin structure (2.17) leads to

$$\chi_a = \frac{1}{2}[\chi_+ + \chi_-] , \quad \chi_p = \chi_- \quad \leftrightarrow \quad \chi_+ = 2\chi_a - \chi_p , \quad \chi_- = \chi_p . \quad (2.21)$$

The arguments of these matrices are $(\mathbf{r}_1|\mathbf{r}'_1, \mathbf{r}_2|\mathbf{r}'_2)$. Their diagonals $(\mathbf{r}_1|\mathbf{r}_1, \mathbf{r}_2|\mathbf{r}_2)$ determine the normalizations

$$\alpha^3 \int_0^\infty d(r_{12}^3) \frac{1}{2} \chi_a = 0, \quad \alpha^3 \int_0^\infty d(r_{12}^3) \frac{1}{2} \chi_p = c \quad \leftrightarrow \quad \alpha^3 \int_0^\infty d(r_{12}^3) \frac{1}{2} \chi_\pm = \mp c. \quad (2.22)$$

The singlet/triplet matrices χ_\pm define symmetric and antisymmetric cumulant geminals $\psi_K^\pm(\mathbf{r}_1, \mathbf{r}_2)$ with corresponding weights ν_K^\pm and with $\Sigma_K \nu_K^\pm = \mp c$ as total weights. Which properties do these geminals have? Are they discrete (bound) or/and continuous (scattering) states, the latter with phase shifts? Is there a kind of an aufbau principle for the ν_K^\pm ?

2.4 Linked Diagrams

As mentioned above, the cumulant 2-matrices χ_\pm are given by linked diagrams. To each symmetrized direct diagram $d_1 \hat{=} \chi_{d_1}(\mathbf{r}_1|\mathbf{r}'_1, \mathbf{r}_2|\mathbf{r}'_2)$, d_2, \dots with 2 open particle-hole lines (one running from \mathbf{r}'_1 to \mathbf{r}_1 and another one from \mathbf{r}'_2 to \mathbf{r}_2) belongs an exchange diagram $x_1 \hat{=} \chi_{x_1}(\mathbf{r}_1|\mathbf{r}'_1, \mathbf{r}_2|\mathbf{r}'_2) = \chi_{d_1}(\mathbf{r}_1|\mathbf{r}'_2, \mathbf{r}_2|\mathbf{r}'_1)$, x_2, \dots , such that for $\mathbf{r}'_2 = \mathbf{r}_2$ and $\int d^3 r_2$ there is only one line running from \mathbf{r}'_1 to \mathbf{r}_1 (like the diagrams of the self-energy Σ , cf [12]). With these building elements $\chi_d = \chi_{d_1} + \chi_{d_2} + \dots$ and $\chi_x = \chi_{x_1} + \chi_{x_2} + \dots$ the singlet/triplet components are $\chi_\pm = \chi_d \pm \chi_x$ and from (2.21) follow the decisive relations

$$\chi_a = \chi_d, \quad \chi_p = \chi_d - \chi_x \quad \curvearrowright \quad \chi_\pm = \chi_d \pm \chi_x, \quad (2.23)$$

again with the arguments $(\mathbf{r}_1|\mathbf{r}'_1, \mathbf{r}_2|\mathbf{r}'_2)$. The spin-averaged sum χ can be written as

$$\chi = \frac{1}{2}[\chi_a + \chi_p] \quad \text{or} \quad \chi = \frac{1}{4}\chi_+ + \frac{3}{4}\chi_- \quad \text{or} \quad \chi = \chi_d - \frac{1}{2}\chi_x. \quad (2.24)$$

The a- and p-components are equally weighted, whereas the singlet- and triplet-components have the weights 1/4 and 3/4, and the d-and x-components have the "weights" 1 and -1/2, respectively. From Eqs.(2.23) and (2.24) follow corresponding relations for the PDs $g_{a,p}$ and their cumulant correspondings $h_{a,p}$. Note that for their FTs $S_{a,p}$ and $C_{a,p}$ it holds $S = S_a + S_p$ and $C = C_a + C_p$.

Now the question is: how real physical properties like the PD's $g_{a,p}(r)$ (by taking the *diagonal* elements) as well as the MD $n(k)$ (by Fourier transforming the contracted *off-diagonal* elements) follow from the (more formal) key quantities $\chi_{a,p}$, respectively $\chi_{d,x}$.

2.5 Pair Densities and Structure Factors

With the cumulant PDs $h_a(r_{12}) = \chi_a(\mathbf{r}_1|\mathbf{r}_1, \mathbf{r}_2|\mathbf{r}_2)$ and $h_p(r_{12}) = \chi_p(\mathbf{r}_1|\mathbf{r}_1, \mathbf{r}_2|\mathbf{r}_2)$ and their Fourier transforms $C_{a,p}(q)$ following from (1.9) and (1.10), the PDs $g_{a,p}(r)$ and SFs $S_{a,p}(q)$ are given by (1.6)-(1.8). This shows that for the spin-parallel quantities, the functions $f^2(r)$ and its FT $F(q)$ are needed, cf App.B. So from the cumulant 2-matrices $\chi_{a,p}(\mathbf{r}_1|\mathbf{r}'_1, \mathbf{r}_2|\mathbf{r}'_2)$ follow not only the spin-antiparallel PD $g_a(r)$, but also the spin-parallel PD $g_p(r)$ (supposed the MD $n(k)$ has been calculated first, cf next paragraph). Rigorous theorems for $C_{a,p}(q \rightarrow 0)$, $C_{a,p}(q \rightarrow \infty)$, and $\int_0^\infty d(q^3)C_{a,p}(q)$ are summarized in App.B.

2.6 Contraction Sum Rule and Momentum Distribution

In terms of the Löwdin function $c(k) = n(k)[1-n(k)]$ and of the contracted cumulant matrix (the notation $\hat{\chi} \hat{\curvearrowright}$ means $\mathbf{r}'_2 = \mathbf{r}_2$ and $\int d^3r_2 \dots$)

$$\hat{\chi}_\pm(\mathbf{r}_1|\mathbf{r}'_1) = \int \frac{d^3r_2}{2 \cdot 3\pi^2} \chi_\pm(\mathbf{r}_1|\mathbf{r}'_1, \mathbf{r}_2|\mathbf{r}_2) \quad \hat{\curvearrowright} \quad \hat{\chi}_\pm(k) = \int \frac{d^3r_{11'}}{2 \cdot 3\pi^2} e^{-i\mathbf{k}\mathbf{r}_{11'}} \hat{\chi}_\pm(\mathbf{r}_1|\mathbf{r}'_1) \quad (2.25)$$

the contraction SR (2.19) can be written as $\hat{\chi}_\pm(k) = \mp c(k)$. If the expressions (2.21) and (2.23) are contracted and Fourier transformed, then

$$\hat{\chi}_d(k) = \frac{1}{2}[-c(k) + c(k)] = 0, \quad \hat{\chi}_x(k) = \frac{1}{2}[-c(k) - c(k)] = -c(k). \quad (2.26)$$

This is the contraction SR, which allows to calculate $n(k)$ from

$$\hat{\chi}_x(k) = \int \frac{d^3r_{11'}}{2 \cdot 3\pi^2} e^{-i\mathbf{k}\mathbf{r}_{11'}} \int \frac{d^3r_2}{2 \cdot 3\pi^2} \chi_x(\mathbf{r}_1|\mathbf{r}'_1, \mathbf{r}_2|\mathbf{r}_2), \quad (2.27)$$

supposed χ_x is approximately known. The 'direct' diagrams $\hat{\chi}_d(k)$ with 2 lines do not contribute to $n(k)$, which alone derives from the 1-line diagram $\hat{\chi}_x(k)$. If $n_0(k) = \Theta(1-k)$ means the MD of the ideal Fermi gas, then $n(k) = n_0(k) + \Delta n(k)$ defines its interaction induced correction $\Delta n(k) \geq 0$ for $k \geq 1$ being normalized as $\int d^3k \Delta n(k) = 0$. Thus the contraction SR (2.26) reads finally

$$\mp \Delta n(k) + [\Delta n(k)]^2 = \hat{\chi}_x(k) \quad \text{for } k \geq 1, \quad (2.28)$$

what simplifies as $\Delta n(k \geq 1) \approx \mp \hat{\chi}_x(k)$ for small correlation tails $\Delta n(k)$, as this is the case for the RPA with $\hat{\chi}_x(k) = \hat{\chi}_{xr}(k) + \dots$ and $\Delta n(k) = \Delta n_r(k) + \dots$. The ellipsis mean beyond-RPA terms. From a diagrammatical point of view one may expect, that already

$\hat{\chi}_x(k)$ is the MD, but this is not the case: as derived above, a factor $\text{sign}(1-k)$ has to be added, to transform $\hat{\chi}_x(k)$ to $\Delta n(k)$. So contraction means $\mathbf{r}'_2 = \mathbf{r}_2$, $\int d^3r_2$ and adding a factor $\text{sign}(1-k)$. - From $\Delta n(k)$ follows the Löwdin parameter c , which fixes some CSFs at long wavelengths: $C_x(0) = -c$, $C_p(0) = +c$, and $C(0) = c$.

2.7 Energies

From $\Delta n(k)$ follows the kinetic correlation energy $\Delta t = \int_0^\infty d(k^3) \Delta n(k) k^2 / 2$. The same $\Delta n(k)$ makes $\Delta F = F - F_0$ with (B.18). This allows to calculate the interaction energy $v = v_{\text{HF}} + v_c$, which is built up from the HF part $v_{\text{HF}} = v_0 + \Delta v_{\text{HF}}$ and the cumulant part v_c :

$$v_0 = - \int_0^\infty \frac{d(q^3)}{3 \cdot 4} \frac{1}{2} F_0(q) v(q) , \quad \Delta v_{\text{HF}} = - \int_0^\infty \frac{d(q^3)}{3 \cdot 4} \frac{1}{2} \Delta F(q) v(q) , \quad v_c = - \int_0^\infty \frac{d(q^3)}{3 \cdot 4} C(q) v(q) . \quad (2.29)$$

$v_0 = -\alpha r_s / (4\pi/3)$ is the HF energy in lowest order. $C = C_a + C_p$ is the FT of $h = [h_a + h_p] / 2$, cf (1.9) and (1.10). The cumulant interaction energy $v_c = v_a + v_p$ is part of the interaction correlation energy $v_{\text{corr}} = \Delta v_{\text{HF}} + v_c$. Thus, the energy-components t and v are available, defining the total energy $e = t + v$ as a function of r_s with $v = r_s de / dr_s$ and $t = e - v$. The correlation energy is $e_{\text{corr}} = \Delta t + \Delta v_{\text{HF}} + v_c$.

2.8 Summary of Sec. II

If $\chi_{\pm}(\mathbf{r}_1 | \mathbf{r}'_1, \mathbf{r}_2 | \mathbf{r}'_2)$ is given in terms of diagrams d_1, d_2, \dots with 2 not-closed particle-hole lines (e.g. Fig.2a) and corresponding exchange terms x_1, x_2, \dots (e.g. Figs.3a, 5a), then:

- (i) it follows $n(k)$ from the contraction SR (2.30) and from $n(k)$ it follows t via (1.2).
- (ii) $F(q)$ and $f^2(r)$, which are needed for v_{HF} and $g_p(r)$, respectively, follow also from $n(k)$, cf App.B.
- (iii) $h_{a,p}(r)$ and $C_{a,p}(q)$ and the cumulant interaction energy v_c follow from $\chi_{a,p}$.
- (iv) Finally, $g_a(r) = 1 - h_a(q)$ and $g_p(r) = 1 - f^2(r) - h_p(r)$.

The resulting quantities are the GS-energies t , $v = v_{\text{HF}} + v_c$, $e = t + v$ as functions of r_s and the MD $n(k)$ as well as the PDs $g_{a,p}(r)$ for the many-body quantum kinematics on the lowest level.

III. THE LOWEST-ORDER CUMULANT 2-MATRIX IN RPA

In the following, these basic definitions and relations are applied to the spin-unpolarized HEG in the high-density limit $r_s \rightarrow 0$, as an illustrative example. All linked-diagram (direct and corresponding exchange) terms are taken into account, which contribute in the energy to terms $\sim r_s^2[\ln r_s + \text{const} + O(r_s)]$. These diagrams are shown in Figs.2a, 3a, 4a, 5a.

3.1 The direct building block χ_{d} in RPA

χ_{dr} denotes the direct cumulant 2-matrix χ_{d} in its ring-diagram approximation of Fig.2a: $\chi_{\text{d}} = \chi_{\text{dr}} + \Delta\chi_{\text{d}}$ with an unknown (hopefully small) correction $\Delta\chi_{\text{d}}$ beyond RPA. In its position representation, this χ_{dr} is given by

$$\chi_{\text{dr}}(\mathbf{r}_1|\mathbf{r}'_1, \mathbf{r}_2|\mathbf{r}'_2) = \frac{9}{2} \int \frac{d^3q}{4\pi} \frac{1}{2} \left\{ \int \frac{d\eta}{2\pi i} v(q, \eta) \hat{Q}_1(q, \eta) \hat{Q}_2(q, -\eta) e^{i(\mathbf{k}_1 \mathbf{r}_{11'} - \mathbf{k}_2 \mathbf{r}_{22'} + \mathbf{q} \mathbf{r}_{12})} + \text{h.c.} \right\} \quad (3.1)$$

with the short-hands $\mathbf{r}_{12} = \mathbf{r}_1 - \mathbf{r}_2$ and $\mathbf{r}_{11'} = \mathbf{r}_1 - \mathbf{r}'_1$. The integral operator $\hat{Q}_i(q, \eta)$ generalizes the particle-hole propagator $Q(q, \eta)$, cf (C.4). The diagonal elements $\chi_{\text{dr}}(\mathbf{r}_1|\mathbf{r}_1, \mathbf{r}_2|\mathbf{r}_2) = h_{\text{dr}}(r_{12})$ define a function

$$h_{\text{dr}}(r) = \frac{9}{2} \int \frac{d^3q}{4\pi} q \frac{\sin qr}{qr} \int_0^\infty \frac{du}{\pi} R^2(q, u) w(q, u), \quad (3.2)$$

which contributes with the RPA-beyond term Δh_{d} to the CPD, $h_{\text{d}} = h_{\text{dr}} + \Delta h_{\text{d}}$. When going from (3.1) to (3.2), the contour integration $\eta \rightarrow iqu$, which replaces simultaneously the frequency integration by a velocity integration, leads to the real function $R(q, u) = Q(q, iqu)$ for the particle-hole propagator, cf eg [12], Eq.(B.1). The effective interaction $w(q, u) = v(q, iqu) = v(q)/[1 + v(q)R(q, u)] = q_c^2/[q^2 + q_c^2 R(q, u)]$ is the RPA screened Coulomb interaction with a Yukawa-like cut-off $q_c^2 R(q, u)$. The qualitative behavior of $h_{\text{a}} = h_{\text{d}}$ is in [5], Fig.3; it starts at $h_{\text{a}}(0) = c_1$ and decays, passes a zero-intercept and approaches 0 from below, its normalization is zero, see (B.1). The FT of $h_{\text{dr}}(r)$, namely

$$C_{\text{dr}}(q) = \int \frac{d^3r}{3\pi^2} \cos \mathbf{q} \mathbf{r} \frac{1}{2} h_{\text{dr}}(r) = \frac{3}{2\pi} q \int_0^\infty du R^2(q, u) w(q, u), \quad (3.3)$$

contributes to the CSF $C_{\text{d}} = C_{\text{dr}} + \Delta C_{\text{d}}$ [29] with a beyond-RPA term ΔC_{d} . How does $C_{\text{dr}}(q)$ behave for small and large momentum transfers, $q \ll q_c$ and $q \rightarrow \infty$, respectively,

and in between ?

For small $q \ll q_c$, the dynamic RPA-propagator $R(q, u)$ can be approximated by its static truncation $R_0(u) = 1 - u \arctan(1/u)$ [29] such that $C_{\text{dr}}(q \ll q_c) = L(y) q_c/2$ with $y = q/q_c$ and

$$L(y) = \frac{3}{\pi} \int_0^\infty du \frac{R_0^2(u)}{y + \frac{1}{y} R_0(u)} = \frac{3}{4}y - \frac{\sqrt{3}}{2}y^2 - \frac{\sqrt{3}}{2}y^2\varphi(y), \quad \varphi(y) = -\frac{9}{10}y^2 + \frac{3}{5}y^3 + \dots \quad (3.4)$$

(For the properties of $L(y)$ see [6].) Thus

$$C_{\text{dr}}(q \ll q_c) = z_{\text{F}}^2 \frac{3q}{8} - \frac{q^2}{4\omega_{\text{pl}}} - \frac{q^2}{4\omega_{\text{pl}}} \varphi\left(\frac{q}{q_c}\right) + \dots, \quad (3.5)$$

in agreement with [35–37]. The ellipsis represents terms originating from the difference $\Delta R(q, u) = R(q, u) - R_0(u)$. The function $C_{\text{dr}}(q)$ starts linearly in a small region ($q \ll q_c$), which shrinks and finally vanishes for $r_s \rightarrow 0$. The beyond-RPA factor z_{F}^2 is added by hand with the following argument. As shown in [53], the small- q behavior of the HF-function $F(q)$ is given in (B.18). It transfers via the SFs to the CSFs and [together with the assumption $\Delta C_{\text{d}}(q \ll q_c) = -z_{\text{F}}^2 q^3/32 + O(q^4)$] makes them behave correctly for small q , according to the plasmon SR (B.3) and (B.13), see also Table 1 and 2.

At the other end, the large- q asymptotics does not require the ring diagram summation, so perturbation theory holds and the "descreening" replacement $w(q, u) \approx v(q)$ is possible. With the Macke function $I(q) = 8\pi q \int_0^\infty du R^2(q, u)$ (explicitly given in [9]) it is

$$C_{\text{dr}}(q \rightarrow \infty) = \frac{I(q)}{(4\pi/3)^2} \frac{\omega_{\text{pl}}^2}{q^2} + O(\omega_{\text{pl}}^4), \quad \frac{I(q)}{(4\pi/3)^2} = \frac{1}{q^2} + \frac{2}{5} \frac{1}{q^4} + O\left(\frac{1}{q^6}\right), \quad \omega_{\text{pl}}^2 = \frac{q_c^2}{3}. \quad (3.6)$$

"In between" $q \rightarrow 0$ and $q \rightarrow \infty$ and according to (1.9), the integral $c_{\text{dr}} = \int_0^\infty d(q^3) C_{\text{dr}}(q)$ contributes to the correlation parameter $c_1 = c_{\text{dr}} + \dots$, where the ellipsis represents the missing terms beyond RPA. The behavior of $C_{\text{d}} = C_{\text{dr}} + \Delta C_{\text{d}}$ with the RPA-beyond term ΔC_{d} (causing the correlation parameters $c_{1,2}$) is summarized in line 1 of Table 1 with unknown coefficients $s_{4,5}$.

3.2 The exchange building block χ_x in RPA

As stressed by Geldart et al. [33], for a consistent small- r_s description the leading exchange

terms of $n_x(k)$, $S_x(q)$ are needed. They follow from χ_x with the ring-diagram part χ_{xr} (Fig. 3a): $\chi_x = \chi_{\text{xr}} + \Delta\chi_x$ with an unknown (hopefully small) correction $\Delta\chi_x$ beyond RPA. That exchange contribution χ_{xr} , which corresponds to the above χ_{dr} , arises from the exchange $\mathbf{r}'_1 \leftrightarrow \mathbf{r}'_2$, i.e. from $\chi_{\text{xr}}(\mathbf{r}_1|\mathbf{r}'_1, \mathbf{r}_2|\mathbf{r}'_2) = \chi_{\text{dr}}(\mathbf{r}_1|\mathbf{r}'_2, \mathbf{r}_2|\mathbf{r}'_1)$, thus

$$\chi_{\text{xr}}(\mathbf{r}_1|\mathbf{r}'_1, \mathbf{r}_2|\mathbf{r}'_2) = \frac{9}{2} \int \frac{d^3q}{4\pi} \frac{1}{2} \left\{ \int \frac{d\eta}{2\pi i} \hat{Q}_1(q, \eta) \hat{Q}_2(q, -\eta) v(q, \eta) e^{i(\mathbf{k}_1 \mathbf{r}_{12'} - \mathbf{k}_2 \mathbf{r}_{21'} + \mathbf{q} \mathbf{r}_{12})} + \text{h.c.} \right\}. \quad (3.7)$$

The diagonal elements $h_{\text{xr}}(r_{12}) = \chi_{\text{xr}}(\mathbf{r}_1|\mathbf{r}_1, \mathbf{r}_2|\mathbf{r}_2)$ define a function

$$h_{\text{xr}}(r) = \frac{9}{2} \int \frac{d^3q}{4\pi} \text{Re} \int \frac{d\eta}{2\pi i} \hat{Q}_1(q, \eta) \hat{Q}_2(q, -\eta) v(q, \eta) \frac{\sin kr}{kr} \Big|_{\mathbf{k}=\mathbf{k}_1+\mathbf{k}_2+\mathbf{q}}, \quad (3.8)$$

which contributes to the CPD $h_x = h_{\text{xr}} + \Delta h_x$. Its FT

$$C_{\text{xr}}(q) = \int \frac{d^3r}{3\pi^2} \cos \mathbf{q} \mathbf{r} \frac{1}{2} h_{\text{xr}}(r) = \frac{3}{2} \text{Re} \int \frac{d\eta}{2\pi i} \hat{Q}_1(k, \eta) \hat{Q}_2(k, -\eta) v(k, \eta) \Big|_{\mathbf{k}=\mathbf{k}_1+\mathbf{k}_2+\mathbf{q}}$$

contributes to the CSF $C_x = C_{\text{xr}} + \Delta C_x$ with the RPA-beyond term ΔC_x . A careful study shows, that C_{xr} can be written as

$$C_{\text{xr}}(q) = \frac{\omega_{\text{pl}}^2}{(4\pi/3)^2} \int d^3k_1 d^3k_2 \int \frac{k du}{\pi} \frac{\varepsilon_1 \varepsilon_2}{(k^2 u^2 + \varepsilon_1^2)(k^2 u^2 + \varepsilon_2^2)} \cdot \frac{1}{k^2 + q_c^2 R(k, u)}, \quad (3.9)$$

$k_{1,2} < 1, \quad |\mathbf{k}_{1,2} + \mathbf{q}| > 1, \quad \mathbf{k} = \mathbf{k}_1 + \mathbf{k}_2 + \mathbf{q}, \quad \varepsilon_1 = t(\mathbf{k}_2 + \mathbf{q}) - t(\mathbf{k}_1), \quad \varepsilon_2 = t(\mathbf{k}_1 + \mathbf{q}) - t(\mathbf{k}_2).$

This is the exchange counterpart to the direct CSF (3.3), unfortunately not known as an explicit function of q . If one assumes for the small- q behavior $C_{\text{xr}}(q \ll q_c) = O(q^4)$ and $\Delta C_x(q \ll q_c) = -c + O(q^4)$, then the correct small- q behavior of $C_p = C_d - C_x$ and S_p results, namely $C_p(0) = c$, see (B.2), and consequently $S_p(0) = 0$, see (1.4). Line 2 of Table 1 contains so far unknown coefficients $s'_{4,5}$. At the other end, the large- q asymptotics of $C_{\text{xr}}(q)$ can be extracted from perturbation theory, replacing "r" by its lowest order "1". This allows the u -integration, by which appears the well-known energy denominator:

$$\int \frac{dx}{\pi} \frac{\varepsilon_1 \varepsilon_2}{(x^2 + \varepsilon_1^2)(x^2 + \varepsilon_2^2)} = \frac{1}{\varepsilon_1 + \varepsilon_2} = \frac{1}{\tau_1 + \tau_2} = \frac{1}{\mathbf{q}(\mathbf{k}_1 + \mathbf{k}_2 + \mathbf{q})}.$$

Thus, it results similar as $C_{\text{dr}}(q \rightarrow \infty)$, namely

$$C_{\text{xr}}(q \rightarrow \infty) = \frac{I_x(q)}{(4\pi/3)^2} \frac{\omega_{\text{pl}}^2}{q^2} + O(\omega_{\text{pl}}^4), \quad \frac{I_x(q \rightarrow \infty)}{(4\pi/3)^2} = \frac{1}{q^2} + \frac{x}{q^4} + O\left(\frac{1}{q^6}\right) \quad (3.10)$$

with an unknown coefficient x . For $I_x(q)$ in general and possibly $x = 8/5$, see App.C. The behavior of $C_x = C_{\text{xr}} + \Delta C_x$ is summarized in line 2 of Table 1. An additional correlation

parameter c'_2 arises from the RPA-beyond term ΔC_x .

3.3 How the cumulant structure factors $C_{a,p}$ follow from $C_{d,x}$

For the spin-antiparallel structure factors it holds $C_a = C_d$. In RPA, $C_d(q)$ is given by (3.3) and its large- q asymptotics is given by (3.6). But beyond RPA the electron-electron coalescing cusp theorem $h'_a(0) = -\alpha r_s[1 - h_a(0)]$ (App.B1, [31]) makes the first term decorated with an additional factor $1 - c_1 = 1 - h_a(0) < 1$. One may expect the next term is modified in a similar way, thus

$$C_a(q \rightarrow \infty) = (1 - c_1) \frac{\omega_{\text{pl}}^2}{q^4} + \left(\frac{2}{5} + c_2 \right) \frac{\omega_{\text{pl}}^2}{q^6} + \dots, \quad \omega_{\text{pl}}^2 = \frac{4\alpha r_s}{3\pi} \quad (3.11)$$

with unknown correlation parameters $c_{1,2}$ vanishing for $r_s \rightarrow 0$. Note that the spin-antiparallel CSF $C_a(q \rightarrow \infty)$ starts with $1/q^4$.

For the spin-parallel structure factors it holds $C_p = C_d - C_x$, $C_{\text{pr}} = C_{\text{dr}} - C_{\text{xr}}$, and $\Delta C_p = \Delta C_d - \Delta C_x$. The large- q asymptotics of $C_x(q)$ is conjectured as (with another correlation parameter c'_2)

$$C_x(q \rightarrow \infty) = (1 - c_1) \frac{\omega_{\text{pl}}^2}{q^4} + (x + c'_2) \frac{\omega_{\text{pl}}^2}{q^6} + \dots, \quad (3.12)$$

such that the difference $C_d - C_x = C_p$ starts asymptotically according to

$$C_p(q \rightarrow \infty) = \left(\frac{2}{5} - x + c_2 - c'_2 \right) \frac{\omega_{\text{pl}}^2}{q^6} + \dots \quad (3.13)$$

with $1/q^6$ (not with $1/q^4$). Just this conclusion results also from the electron-electron coalescing curvature theorem with $x = 8/5$, cf (B.7). At the other end, the small- q behavior $C_p(q \ll q_c)$ follows from the above derived/assumed expressions for $C_d(q \ll q_c)$ and $C_x(q \ll q_c)$:

$$C_p = C_d - C_x = c + z_F^2 \left(\frac{3q}{8} - \frac{q^3}{16} \right) - \frac{q^2}{4\omega_{\text{pl}}} + \left[s_4'' \left(\frac{q}{\omega_{\text{pl}}} \right)^4 + s_5'' \left(\frac{q}{\omega_{\text{pl}}} \right)^5 + \dots \right] \omega_{\text{pl}}. \quad (3.14)$$

[For the qualitative behavior of the corresponding CPD h_p see [5], Fig.4; it starts with $h_p(r \ll r_c) = (c_3/2)r^2 + \dots$, see (B.2), (B.5), (B.8).] A consequence for the total CSF $C = C_a + C_p = 2C_d - C_x$ is

$$C(q \ll q_c) = c + z_F^2 \left(\frac{3q}{4} - \frac{q^3}{16} \right) - \frac{q^2}{2\omega_{\text{pl}}} + \left[s_4''' \left(\frac{q}{\omega_{\text{pl}}} \right)^4 + s_5''' \left(\frac{q}{\omega_{\text{pl}}} \right)^5 + \dots \right] \omega_{\text{pl}} + \dots. \quad (3.15)$$

This, used in $S(q) = 1 - \frac{1}{2}F(q) - C(q) = c + z_F^2(\frac{3q}{4} - \frac{q^3}{16}) - C(q) + \dots$, cancels the first three terms. Thus emerges the quadratic term in agreement with the plasmon SR $S(q \ll q_c) = q^2/(2\omega_{pl}) + \dots$. Consequently an inflexion point appears near the origin. Its trajectory with $r_s \rightarrow 0$ is sketched in App.B. Table 2 gives the small- q and large- q behavior of $S_{a,p}$. For the small- q behavior of $S = S_a + S_p$ the result (B.13) of the inflexion-point analysis with further correlation parameters $c_{4,5}$ is used, see Table 2. It remains open to check the above assumption on $C_x(q \ll q_c)$.

3.4 How v follows from the cumulant structure factor $C = C_a + C_p = 2C_d - C_x$

If (3.3) and (3.9) are used in (2.29), then the cumulant interaction energy $v_c = v_d + v_x = v_{dr} + v_{xr} + \dots$ with ("r" = RPA, ellipsis = beyond RPA)

$$v_{dr} + v_{xr} = -\frac{1}{2} \int \frac{d^3q}{4\pi} v(q) [C_{dr}(q) - \frac{1}{2}C_{xr}(q)] \quad (3.16)$$

consists of a "direct" part v_{dr} and a corresponding "exchange" part v_{xr} . The first one,

$$v_{dr} = -\frac{3}{4\pi} \int \frac{d^3q}{4\pi} q \int_0^\infty du v(q)R^2(q, u)w(q, u) , \quad (3.17)$$

agrees (of course) with what follows from the total energy e after Macke (1950) [14] and Gell-Mann/Brueckner (1957) [15],

$$e_{dr} = -\frac{3}{4\pi} \int \frac{d^3q}{4\pi} q \int_0^\infty du \{v(q)R(q, u) - \ln[1 + v(q)R(q, u)]\} , \quad (3.18)$$

by means of the virial theorem $v = r_s de/dr_s$. The "exchange" part v_{xr} can be simplified as

$$v_{xr} = +\frac{1}{4} \int \frac{d^3q}{4\pi} v(q)C_{x1}(q) + \dots , \quad C_{x1}(q) = \frac{3}{(4\pi)^2} I_x(q)v(q) . \quad (3.19)$$

Namely, whereas in $C_{xr}(q)$ the screened interaction $v(q, \eta)$ is necessary to remove the long-range divergencies of the bare interaction $v(q)$, this is not the case for v_{x2} , which has been calculated by Onsager/Mittag/Stephen (1966) [38] with the result

$$v_{x2} = \frac{3}{4} \int \frac{d^3q}{(4\pi)^3} v^2(q)I_x(q) = 2 \left[\frac{1}{6} \ln 2 - \frac{3}{4} \frac{\zeta(3)}{\pi^2} \right] (\alpha r_s)^2 . \quad (3.20)$$

Note that $v_{x2} = 2 e_{x2}$.

The agreement of (3.18) with the results of Macke and Gell-Mann/Brueckner [14, 15] and of (3.20) with the calculations of Onsager et al. [38] confirms also the above expressions for $h_{a,p}(r)$ and $C_{a,p}(q)$ in the RPA approximations "dr" and "xr".

3.5 How n_r follows from the contraction of χ_{xr}

From χ_{xr} of (3.7) follows also a contribution to

$$\hat{\chi}_x(k) = \hat{\chi}_{xr}(k) + \dots, \quad \hat{\chi}_{xr}(k) = \int \frac{d^3 r_{11'}}{2 \cdot 3\pi^2} e^{-i\mathbf{k}\mathbf{r}_{11'}} \int \frac{d^3 r_2}{2 \cdot 3\pi^2} \chi_{xr}(\mathbf{r}_1|\mathbf{r}'_1, \mathbf{r}_2|\mathbf{r}_2). \quad (3.21)$$

As explained in App.D, the MD $n(k)$ starts with a 2nd-order term, hence $v(q, \eta)$ can be replaced by $-v(q)Q(q, \eta)v(q, \eta)$. Therefore

$$\begin{aligned} \chi_{xr}(\mathbf{r}_1|\mathbf{r}'_1, \mathbf{r}_2|\mathbf{r}_2) &= \frac{9}{2} \int \frac{d^3 q}{4\pi} \frac{1}{2} \left\{ \int \frac{d\eta}{2\pi i} [-v(q)Q(q, \eta)v(q, \eta)] \cdot \right. \\ &\cdot \hat{Q}_1(q, \eta)\hat{Q}_2(q, -\eta) e^{-i(\mathbf{k}_1+\mathbf{k}_2+\mathbf{q})\mathbf{r}_2} e^{i[(\mathbf{k}_1+\mathbf{q})\mathbf{r}_1+\mathbf{k}_2\mathbf{r}'_1]} + \text{h.c.} \left. \right\}. \end{aligned} \quad (3.22)$$

The \mathbf{r}_2 -integration and afterwards the $\mathbf{r}_{11'}$ -integration yield (including prefactors)

$$\left(\frac{(2\pi)^3}{2 \cdot 3\pi^2} \right)^2 \delta(\mathbf{k}_1 + \mathbf{k}_2 + \mathbf{q}) \delta(\mathbf{k} + \mathbf{k}_2) = \left(\frac{4\pi}{3} \right)^2 \delta(\mathbf{k}_1 + \mathbf{q} - \mathbf{k}) \delta(\mathbf{k}_2 + \mathbf{k}), \quad (3.23)$$

so that

$$\hat{\chi}_{xr}(k) = -\frac{1}{2} \int \frac{d^3 q}{4\pi} \frac{1}{2} \left\{ \int \frac{d\eta}{2\pi i} v(q)Q(q, \eta)v(q, \eta)X(q, \eta) + \text{c.c.} \right\} \quad (3.24)$$

with

$$X(q, \eta) = 4\pi \hat{Q}_1(q, \eta)\delta(\mathbf{k}_1 + \mathbf{q} - \mathbf{k}) \cdot 4\pi \hat{Q}_2(q, -\eta)\delta(\mathbf{k}_2 + \mathbf{k}) = \frac{\tilde{\Theta}(\mathbf{k}, \mathbf{q})}{[\tau(\mathbf{k}, \mathbf{q}) - \eta]^2}, \quad (3.25)$$

where $\tilde{\Theta}(\mathbf{k}, \mathbf{q}) = 1$ for $|\mathbf{k}| \geq 1, |\mathbf{k}+\mathbf{q}| \leq 1$ and 0 otherwise. The last step is derived in App.C4.

This used in (3.24) gives for the MD-correlation part the result $\Delta n(k) = n_r(k) + \dots$ with

$$n_r(k \geq 1) = \pm \frac{1}{2} \int \frac{d^3 q}{4\pi} \frac{1}{2} \left\{ \int \frac{d\eta}{2\pi i} v(q)Q(q, \eta)v(q, \eta) \frac{\tilde{\Theta}(\mathbf{k}, \mathbf{q})}{[\tau(\mathbf{k}, \mathbf{q}) - \eta]^2} + \text{c.c.} \right\}. \quad (3.26)$$

With $\Theta(\mathbf{k}, \mathbf{q}) = \pm \tilde{\Theta}(\mathbf{k}, \mathbf{q})$ for $|\mathbf{k}| \geq 1$ and again with $\eta \rightarrow iqu$, it turns out

$$n_r(k) = \frac{1}{2} \int_0^\infty d(q^2) \int_0^\infty \frac{du}{2\pi} v(q)R(q, u)w(q, u) \operatorname{Re} \int_{-1}^{+1} \frac{d\zeta}{2} \frac{\Theta(\mathbf{k}, \mathbf{q})}{[(k\zeta + \frac{q}{2}) - iu]^2}, \quad (3.27)$$

being ≥ 0 for $k \geq 1$. This is exactly the RPA-MD of Daniel/Vosko (1960) and Kulik (1961), as it has been shown in detail in [12] on the way therein from Eqs.(3.34) to (3.38). Also

therein at (3.10) it is shown, what $n_r(k)$ contributes to the kinetic energy t in agreement with the virial theorem (1.1) and the Macke/Gell-Mann/Brueckner energy (3.18). The asymptotic behavior is $n(k \rightarrow \infty) = \omega_{\text{pl}}^4/(2k^8) + \dots$ for RPA and $n(k \rightarrow \infty) = (1 - c_1)\omega_{\text{pl}}^4/(2k^8) + \dots$ beyond it. This 2nd-order result is reduced by a factor of 1/2 through a still missing ladder diagram in its exchange version, as treated in the next section.

IV. THE 2ND-ORDER 2-MATRIX IN RPA

This ladder diagram has a particle-hole line running from 1' to 2 and a 2nd line from 2' to 1, cf Fig.5a. Its contraction $\mathbf{r}'_2 = \mathbf{r}_2$ and $\int d^3r_2$ yields the diagram of Fig.5b, which differs from Fig.5c only by a factor $\text{sign}(1 - k)$ according to (2.28). In detail the diagram χ_{lxr} of Fig.5a is given by (C.12). If for simplicity the RPA screening is neglected (corresponding to the replacement $r \rightarrow 2$) and a series of laborious contour integrations are carefully performed together with the contraction steps analog (3.21), it finally yields

$$\hat{\chi}_{\text{lx2}}(k) = \frac{1}{4} \int \frac{d^3q_1 d^3q_2}{(4\pi/3)^2} \frac{\omega_{\text{pl}}^4}{q_1^2 q_2^2} \frac{\Theta(\mathbf{k}, \mathbf{q}_{1,2})}{(\mathbf{q}_1 \cdot \mathbf{q}_2)^2} > 0 \quad \rightsquigarrow \quad n_x(k \geq 1) = \mp \hat{\chi}_{\text{lx2}}(k). \quad (4.1)$$

The mentioned factor $\text{sign}(1 - k)$ transforms $\hat{\chi}_{\text{lx2}}(k)$ to the corresponding MD contribution $n_x(k)$, which thus reduces both the particle branch ($k > 1$) and the hole branch ($k < 1$) of the RPA-MD $n_r(k)$, Eq.(3.27). In particular the asymptotics for $k \rightarrow \infty$ changes from 1/2 to 1/4 of ω_{pl}^4/k^8 as already mentioned at the end of Sec.III. Furthermore it is easy to show by means of the substitutions $\mathbf{k} \rightarrow -(\mathbf{k} + \mathbf{q}_1)$ and $\mathbf{q}_2 \rightarrow -\mathbf{q}_2$, (i) the zero normalization $\int d^3k n_{\text{lx2}}(k) = 0$ and (ii) the kinetic energy

$$t_{\text{lx2}} = \frac{1}{8} \int \frac{d^3k d^3q_1 d^3q_2}{(4\pi/3)^3} \frac{\omega_{\text{pl}}^4}{q_1^2 q_2^2} \frac{\Theta^-(\mathbf{k}, \mathbf{q}_{1,2})}{\mathbf{q}_1 \cdot \mathbf{q}_2}, \quad (4.2)$$

where also the identity (C.20) is used. The result (4.2) is just the exchange integral, which has been solved analytically by Onsager et al. [38]. Whereas (4.2) is a non-divergent 2nd-order term, for $n(k \approx 1)$ an indeed complicated ring-diagram summation is needed, to ameliorate diverging terms.

V. SUMMARY AND OUTLOOK

This is a contribution to the theory of extended many-electron systems in terms of reduced-density matrices (RDMs), which replace $\Phi(1, \dots, N)$, the many-electron wave functions of finite systems and form an infinite hierarchy, such that a lower-level RDM follows from the next-higher-level RDM by means of a certain contraction procedure, e.g. from the 2-body matrix (2-matrix) γ_2 follows the 1-matrix γ_1 . This paper is driven by the belief that the **cumulant 2-matrix** γ_c (dimensionless: χ) has a fundamental meaning. This shows up for extended systems (i) in its size-extensive normalization and contraction and (ii) in its (closely related) *linked*-diagram representation. Besides it is a decisive key quantity, because from it follows both the pair density (PD) and the 1-matrix. Here it is aimed to unveil its secrets for the high-density spin-unpolarized homogeneous electron gas (HEG). Although this model is only a marginal corner in the complex field of electron correlation, one should get generally deeper insight into the many-body correlation by exploiting the concept of cumulant decomposition of RDMs. The ground state (GS) energy of an electronic system is a simple functional of $\rho(\mathbf{r}, \sigma)$ = electron density, of $n(\mathbf{k}, s)$ = momentum distribution (MD), and of $g(1, 2)$ = pair density (PD) with $1 = (\mathbf{r}_1, \sigma_1)$. These 1- and 2-body quantities have their common origin in the 2-matrix $\gamma_2(1|1', 2|2')$. Whereas the PD simply follows from γ_2 by taking the diagonal elements, the 1-body quantities need a procedure called contraction which means $2' = 2$ and $\int d2$. But this procedure leads in the case of extended systems to difficulties with the thermodynamic limit (TDL). Namely non-size-extensive expressions $\sim N^2$ appear, resulting from the numbers of pairs $N(N - 1)$. This is avoided by the cumulant decomposition of the 2-matrix γ_2 . This means that γ_2 is additively decomposed into a HF-like (or exact exchange) term γ_{HF} , which reduces to a sum of products of the (correlated) 1-matrix, and a non-reducible remainder, called cumulant matrix γ_c . Its advantage: it is *size-extensively* normalizable and contractable. Thus the problems with the TDL are eliminated. This is worked out in detail for the HEG with the homogeneous electron density ρ , with the MD $n(k)$ and with $S(q)$, the structure factor (SF) [or equivalently the 1-matrix $f(|\mathbf{r}_1 - \mathbf{r}'_1|)$ and the PD $g(r_{12})$, respectively]. The 2-body quantities $S(q)$ and $g(r)$ are decomposed into HF terms and remainders $C(q)$ and $h(r)$, respectively called cumulant SF (CSF) and cumulant PD (CPD). In detail, this means $g(r) = 1 - \frac{1}{2}f^2(r) - h(r)$ and $S(q) = 1 - \frac{1}{2}F(q) - C(q)$ with $F(q)$ = Fourier transform of

$f^2(r)$. The contraction procedure is developed in Eqs.(2.25)-(2.28): A quadratic equation for $\Delta n(k) = n(k) - n_0(k)$ yields the 2 branches for particles ($k > 1$) and holes ($k < 1$).

Closely related to the described *size-extensivity* of the cumulant 2-matrix is its form (within many-body perturbation theory) in terms of *linked* diagrams. Under the impression that the triangle of "cumulants \leftrightarrow size-extensivity \leftrightarrow linked diagrams" is a fundamental relation (with an exponential-linked-diagram theorem as a more general mathematical background [40, 41]), one may curiously ask for the **cumulant geminals** $\psi_K^\pm(\mathbf{r}_1, \mathbf{r}_2)$ and their weights ν_K^\pm , which diagonalize γ_c [42], analogous to Eq.(2.16) in [5]. What are their properties? Is there perhaps a 2-body scheme, which allows to calculate approximately these ψ_K^\pm and ν_K^\pm ? How they differ from the Overhauser geminals [48], which parametrize the PD $g(r)$? One access to this subject are the contracted Schrödinger equations [41]. But instead of this, in this paper the cumulant 2-matrix of the high-density HEG is derived. The results for γ_c (dimensionless χ) prove to be correct, because they yield the known RPA expressions for $S(q)$, $g(r)$, and $n(k)$. This is the 1st step for further curiosity studies along the line of Overhauser [48], namely to find the cumulant geminals of the high-density HEG, to be specific: the expressions (3.1), (3.7), and (C.12) have to be diagonalized.

Furthermore, the coalescing cusp and curvature theorems, the plasmon sum rule (and its consequence, the inflexion-point trajectory), as well as the small- and large- q behavior of the CSFs for electron pairs with parallel and antiparallel spins are systematically summarized (analog to [36]), see Table 1 and 2. Within this, also the so far assumed asymptotic behavior of the structure factors for small and large q is corrected.

Acknowledgments

The author is grateful to P. Gori-Giorgi, Jian Wang, K. Morawetz, J. Bodyfelt for discussions and hints and acknowledges P. Fulde and the Max Planck Institute for the Physics of Complex Systems Dresden for supporting this work and thanks Th. Müller and R. Schuppe for technical help.

Appendix A: Generating functionals and linked diagrams

The most compact quantity containing all the secrets of the HEG GS) is the generating functional

$$\gamma[\eta^\dagger|\eta] = \langle \hat{P} e^{\int dx [\eta^\dagger(x)\psi(x) + \eta(x)\psi^\dagger(x)]} \rangle \quad (\text{A.1})$$

with $x = (\mathbf{r}, \sigma)$ and $\int dx = \sum_\sigma \int d^3r$. $\eta(x)$ and $\eta^\dagger(x)$ are Grassmann variables and \hat{P} makes the normal ordering, i.e. orders the creation operators ψ^\dagger including sign changes to the left. The Volterra coefficients of $\gamma[\eta^\dagger|\eta]$ are the RDMs $\gamma_1, \gamma_2, \dots$. The ansatz $\gamma[\eta^\dagger|\eta] = e^{\chi[\eta^\dagger|\eta]}$ defines another generating functional, $\chi[\eta^\dagger|\eta]$, the Volterra coefficients of which are the so-called cumulant matrices χ_1, χ_2, \dots , such that a hierarchy results with higher level RDMs expressed by sums of products of lower level RDMs and non-reducible remainders. Thus it holds e.g. $\gamma_1(x|x') = \chi_1(x|x')$, $\gamma_2(x_1|x'_1, x_2|x'_2) = \tilde{A}\chi_1(x_1|x'_1)\chi_1(x_2|x'_2) + \chi_2(x_1|x'_1, x_2|x'_2)$, ... with \tilde{A} being an antisymmetrizer [40]. Within time-dependent perturbation theory (S -matrix theory) the cumulant matrices χ_1, χ_2, \dots are given by non-vacuum *linked* diagrams only and closely related to this they are size-extensively normalized i.e. $\int dx_1 dx_2 \dots \chi(x_1|x_1, x_2|x_2, \dots) \sim N$, what allows for extended systems the thermodynamic limit with $N \rightarrow \infty, \Omega \rightarrow \infty, \rho = N/\Omega = \text{const}$ [41].

Appendix B: Structure Factors

Here are summarized the normalizations of $C_{\text{a,p}}(q), C(q)$ etc. as well as their behavior for small and large arguments.

B1: Perfect Screening Sum Rule. Cusp and Curvature Theorems

$S(q)$ starts with $S(0) = 0$ and approaches 1 for $q \rightarrow \infty$. $g(r)$ starts with $g(0) \leq 1/2$ and oscillatory approaches 1 for $r \rightarrow \infty$. Note, that $g_{\text{a,p}}(r) \geq 0 \curvearrowright g(r) \geq 0$, since they are probabilities. The normalizations of $1 - S(q)$ and $1 - g(r)$ are contained in (1.5) with $g(0) = (1 - c_1)/2$ (defining the correlation parameter c_1) and with $S(0) = 0$ (the perfect screening SR), respectively:

$$\int_0^\infty d(q^3) [1 - S(q)] = 1 + c_1, \quad \alpha^3 \int_0^\infty d(r^3) [1 - g(r)] = 1.$$

Similarly, the normalizations of $1 - g_{a,p}(r)$, $S_a(q)$, and $1 - S_p(q)$ are in (1.4) fixed with $g_a(0) = c_1$, $g_p(0) = 0$, and $S_{a,p}(0) = 0$. In terms of cumulant and "a,p" components, this reads as

$$h_a(0) = c_1 \leftrightarrow \int_0^\infty d(q^3) C_a(q) = c_1, \quad C_a(0) = 0 \leftrightarrow \alpha^3 \int_0^\infty d(r^3) \frac{1}{2} h_a(r) = 0, \quad (\text{B.1})$$

$$h_p(0) = 0 \leftrightarrow \int_0^\infty d(q^3) C_p(q) = 0, \quad C_p(0) = c \leftrightarrow \alpha^3 \int_0^\infty d(r^3) \frac{1}{2} h_p(r) = c, \quad (\text{B.2})$$

which follows from the FTs (1.9) and (1.10) for $r = 0$, respectively for $q = 0$. With $\frac{1}{2}F(0) = 1 - c$, the perfect screening SR $S(0) = 0$ is hidden in $C(0) = C_a(0) + C_p(0) = c$. More general is the plasmon SR [17, 18]

$$S(q \ll q_c) = \frac{q^2}{2\omega_{\text{pl}}} + O(q^4), \quad (\text{B.3})$$

see Table 2, last line.

According to the electron-electron coalescing cusp theorem $g'_a(0) = \alpha r_s g_a(0)$ for the spin-antiparallel CPD [31], it holds $h'_a(0) = -\alpha r_s(1 - c_1)$ with

$$c_1 = h_a(0) = \frac{2}{5\pi} (\pi^2 - 3 + 6 \ln 2) \alpha r_s + 2 \left(3 - \frac{\pi^2}{4} \right) \left(\frac{3\alpha}{2\pi} \right)^2 r_s^2 \ln r_s + O(r_s^2) \quad (\text{B.4})$$

[28, 29]. Exactly this high-density behavior of $h(0)$ and $g(0)$ results also from the ladder theory as the best method to treat short-range correlation [43, 44, 54]. By means of the Kimball trick [31] it follows the 1st term of Eq.(3.11), whereas the 2nd term follows from $C_a(q) = C_d(q) \approx C_{\text{dr}}(q)$ and from (3.6). c_2 is another correlation parameter vanishing for $r_s \rightarrow 0$. c_1 appears also in the large- k asymptotics $n(k \rightarrow \infty) = (1 - c_1)\omega_{\text{pl}}^4/(4k^8) + \dots$. Thus short-range correlation determine the large-wave number asymptotics of $n(k)$ [45, 46] and of $C(q)$ [31, 45, 54].

For the spin-parallel quantities, the Pauli principle makes $g_p(0) = g'_p(0) = 0$ or equivalently $h_p(0) = h'_p(0) = 0$. Furthermore the electron-electron coalescing curvature theorem says $g_p'''(0) = \frac{3}{2}\alpha r_s g_p''(0)$ or equivalently $h_p'''(0) = \frac{3}{2}\alpha r_s [2f''(0) + h_p''(0)]$. With $f''(0) = -\frac{2}{3}t$ and with [47]

$$c_3 = h_p''(0) = \frac{1}{35\pi} (4\pi^2 - 5 + 20 \ln 2) \alpha r_s + O(r_s^2 \ln r_s), \quad (\text{B.5})$$

it holds $h_p'''(0) = \alpha r_s (\frac{3}{2}c_3 - 2t)$. This determines the large- q asymptotics of $C_p(q)$ as shown in the following by means of the Kimball trick [31]. First a function $c_p(q) \sim 1/q^8$ is defined through $C_p(q) = a/(1+q^2)^3 + c_p(q)$. Then from the FT (1.10) it follows

$$h_p(r) = a \frac{3\pi}{16} (1+r)e^{-r} + \int_0^\infty d(q^3) c_p(q) \frac{\sin qr}{qr} \quad \curvearrowright \quad h_p'''(0) = a \frac{3\pi}{8} . \quad (\text{B.6})$$

With the above curvature theorem it finally results

$$C_p(q \rightarrow \infty) = (3 c_3 - 4t) \frac{\omega_{\text{pl}}^2}{q^6} + \dots . \quad (\text{B.7})$$

Comparing this with (3.13), the SR $\frac{2}{5} - x + c_2 - c_2' = 3c_3 - 4t$ seems to hold. For $r_s \rightarrow 0$ it takes $t \rightarrow 3/10$, hence $x = 8/5$ [for plausible arguments see text after (C.8)].

Because $C_p(q \rightarrow \infty)$ decays so strong, from (B.6) it follows in addition to (B.3) the relation

$$c_3 = h_p''(0) = - \int_0^\infty dq q^4 C_p(q) . \quad (\text{B.8})$$

Since $h_p''(0) > 0$, cf [32, 47], the integral has to be negative. This is in agreement with (B.3) and (B.7): a factor q^2 in front of $C_p(q)$ makes the integral vanishing, cf (B.3). An additional factor q^2 enhances the negative asymptotic branch of $C_p(q \rightarrow \infty)$, cf (B.7). Besides, from $g_p''(0) > 0$ it follows $h_p''(0) < 4t/3$. For $t(r_s)$ cf eg [22].

B2: Plasmon SR and inflexion-point trajectory

In (3.5) it has been shown how perturbation theory and RPA makes the plasmon-term $\sim q^2$ arise from the linear term $\sim q$ of the non-interacting system. Here it is asked on the contrary, if the interaction is switched off ($r_s \rightarrow 0$), how the quadratic behavior $\sim q^2$ is transformed to the linear behavior $\sim q$. The answer: if $S(q)$ starts for small q according to the plasmon SR [18] quadratically with q^2 , then there must be - already from a topological point of view - an inflexion point q_0 , $S(q_0)$, which moves with $r_s \rightarrow 0$ towards the origin. So also the linear behavior at the inflexion point is transported to the origin, realizing thus the correct behavior of the unperturbed ideal Fermi gas, as it should. Now this qualitative discussion is quantized by the ansatz

$$S(q \ll q_c) = \frac{q^2}{2\omega_{\text{pl}}} [1 - az^2 + bz^3 + \dots] , \quad z = \frac{q}{\omega_{\text{pl}}} \quad (\text{B.9})$$

and adjusting the r_s -dependent coefficients a, b appropriately. Namely the power expansion of $S(q)$ around $q \approx q_0$

$$S(q_0 + x) = S(q_0) + \frac{1}{1!}S'(q_0)x + \frac{1}{2!}S''(q_0)x^2 + \frac{1}{3!}S'''(q_0)x^3 + \dots \quad (\text{B.10})$$

is compared with its " $r_s \rightarrow 0$ " limit $S_0(x)$. This gives 3 equations, which allows determining the 3 quantities q_0, a, b :

$$\frac{1}{1!}S'(q_0) \rightarrow \frac{3}{4}, \quad \frac{1}{2!}S''(q_0) = 0, \quad \frac{1}{3!}S'''(q_0) \rightarrow -\frac{1}{16} \quad (\text{B.11})$$

with the result (for $r_s \rightarrow 0$)

$$\frac{q_0}{\omega_{\text{pl}}} \rightarrow \frac{3}{2}, \quad a \rightarrow \frac{1}{3^2}, \quad b \rightarrow \frac{2^2}{3^3 \cdot 5}. \quad (\text{B.12})$$

So (B.9) takes for $r_s \rightarrow 0$ the form (with unknown correlation parameters $c_{4,5}$)[35]

$$S(q \ll q_c) = \frac{q^2}{2\omega_{\text{pl}}} \left[1 - \left(\frac{1}{3^2} + c_4 \right) \left(\frac{q}{\omega_{\text{pl}}} \right)^2 + \left(\frac{2^2}{3^3 \cdot 5} + c_5 \right) \left(\frac{q}{\omega_{\text{pl}}} \right)^3 + \dots \right] + \dots \quad (\text{B.13})$$

Thus the inflexion point moves towards the origin according to $q_0 \rightarrow 1.5 \omega_{\text{pl}}$ and $S(q_0) \rightarrow 0.96 \omega_{\text{pl}}$ with a slope of 0.64 being smaller than $S'_0(0) = 0.75$. Comparison of (B.13) with (3.15) shows $s_4''' = \frac{1}{2}(\frac{1}{3^2} + c_4)$ and $s_5''' = -\frac{1}{2}(\frac{2^2}{3^3 \cdot 5} + c_5)$. - As quoted in [53], other consequences of (B.9) are $g(r \gg r_c) = 1 - 2^5/(\omega_{\text{pl}}^4 r^8) + \dots$ and

$$\alpha^3 \int_0^\infty dr r^4 [1 - g(r)] = \frac{1}{\omega_{\text{pl}}}, \quad \alpha^3 \int_0^\infty dr r^6 [1 - g(r)] = \frac{2^3 \cdot 5}{3^2} \frac{1}{\omega_{\text{pl}}^3}. \quad (\text{B.14})$$

The equation with the weight r^4 is widely used in [37]. Remind $1 - g(r) = \frac{1}{2}f^2(r) + h(r)$, what relates $\int d^3k (dn(k)/dk)^\nu$ to $\int d^3r r^\nu h(r)$ for $\nu = 2$ and $\nu = 4$.

B3: The HF-function $F(q)$

For the spin-parallel quantities $g_p(r) \leftrightarrow S_p(q)$ and $h_p(r) \leftrightarrow C_p(q)$ the functions $f^2(r)$ and its FT $F(q)$ are needed, cf (1.7), (1.8) and Table 2:

$$F(q) = \alpha^3 \int_0^\infty d(r^3) \frac{\sin qr}{qr} f^2(r), \quad \frac{1}{2}F(0) = 1 - c, \quad \int_0^\infty d(q^3) \frac{1}{2}F(q) = 1. \quad (\text{B.15})$$

$F(q)$ transports the MD $n(k)$, as seen from

$$\frac{1}{2}F(q) = \frac{3}{4\pi} \int d^3k n(k)n(|\mathbf{k} - \mathbf{q}|). \quad (\text{B.16})$$

Thus it is related to the probability of finding a pair of electrons with given relative momentum \mathbf{q} [49]. For $r_s = 0$ with $n_0(k) = \Theta(1 - k)$ the integral takes a simple geometric meaning: it is just the volume of two spherical calottes with the height $h = 1 - q/2$, thus $\int d^3k \dots = 2 \cdot \frac{\pi}{3} h^2 (3 - h)$ or

$$\frac{1}{2} F_0(q) = \left[1 - \frac{3q}{2} + \frac{1}{2} \left(\frac{q}{2} \right)^3 \right] \Theta(2 - q), \quad \int_0^\infty d(q^3) \frac{1}{2} F_0(q) = 1. \quad (\text{B.17})$$

[By the way, (i) $F_0(q)$ appears in the Overhauser theory as the weight of its PD geminals [48] and (ii) the singularities of $F(q)$ at $q \rightarrow 0$ and $q \rightarrow 2$ are studied in [53].] The difference $\Delta F(q) = F(q) - F_0(q)$ results from $\Delta n(k) = n(k) - n_0(k)$. It holds

$$\frac{1}{2} \Delta F(q \ll q_c) = -c - z_F^2 \left(\frac{3q}{4} - \frac{q^3}{16} \right) + \dots, \quad \frac{1}{2} \Delta F(q \rightarrow \infty) = \frac{1 - c_1 \omega_{\text{pl}}^4}{8 q^8} + \dots, \quad (\text{B.18})$$

and $\int_0^\infty d(q^3) \Delta F(q) = 0$.

B4: The jump discontinuity of $S''(q)$ and $C''(q)$ at $q = 2$

For transition momenta $|\mathbf{q}| = 2$, when passing this value from below, the topology changes from 2 overlapping to 2 non-overlapping Fermi spheres. The consequence: $\Delta I''(2) = 2\pi^2$, cf (C.2) in [9] $\curvearrowright \Delta C''(2) = (3\omega_{\text{pl}}/4)^2 + \dots$ [6]. The ellipsis represents exchange and beyond-RPA terms. For $S''(2)$ the relation $\frac{1}{2} \Delta F''(2) = -3z_F^2/4$, cf (5.2) in [53], has to be taken into account. Thus in lowest order $\Delta S''(2) = 3z_F^2/4 - (3\omega_{\text{pl}}/4)^2 + \dots$, what causes (in the direct space) the Friedel oscillations of $g(r)$. It remains open to study the exchange term $\Delta I''_x(2)$, which presumably reduces the direct term $\Delta I''(2)$.

Appendix C: Particle-hole propagator and Macke function $I(q)$

C1: The building elements of the RPA Feynman diagrams (cf Figs.2a, 3a, 4a, 5a) are the Coulomb repulsion $v(q) = q_c^2/q^2$ with the coupling constant $q_c^2 = 4\alpha r_s/\pi$ and the one-body Green's function of free electrons with $t(\mathbf{k}) = k^2/2$,

$$G_0(k, \omega) = \frac{\Theta(k - 1)}{\omega - t(\mathbf{k}) + i\delta} + \frac{\Theta(1 - k)}{\omega - t(\mathbf{k}) - i\delta}, \quad \delta \gtrsim 0. \quad (\text{C.1})$$

C2: From $G_0(k, \omega)$ follows the particle-hole propagator $Q(q, \eta)$ in RPA according to

$$Q(q, \eta) = - \int \frac{d^3k}{4\pi} \int \frac{d\omega}{2\pi i} G_0(k, \omega) G_0(|\mathbf{k} + \mathbf{q}|, \omega + \eta) \quad (\text{C.2})$$

with the result

$$Q(q, \eta) = \int \frac{d^3k}{4\pi} \left[\frac{\Theta^+(\mathbf{k}, \mathbf{q})}{\eta - \tau(\mathbf{k}, \mathbf{q}) - i\delta} - \frac{\Theta^-(\mathbf{k}, \mathbf{q})}{\eta - \tau(\mathbf{k}, \mathbf{q}) + i\delta} \right], \quad (\text{C.3})$$

$$\tau(\mathbf{k}, \mathbf{q}) = t(\mathbf{k} + \mathbf{q}) - t(\mathbf{k}) = q \left(k\zeta + \frac{q}{2} \right), \quad \zeta = \cos \sphericalangle(\mathbf{k}, \mathbf{q}).$$

The denominators contain the excitation energy $\tau(\mathbf{k}, \mathbf{q})$, to create a hole with \mathbf{k} inside the Fermi sphere and a particle with $\mathbf{k} + \mathbf{q}$ outside the Fermi sphere. A complicated step function, defined by $\Theta^\pm = 1$ for $k \gtrless 1, |\mathbf{k} + \mathbf{q}| \lesseqgtr 1$ and 0 otherwise, is a consequence of the Pauli principle. $R(q, u) = Q(q, iqu)$ defines a real function. A generalization of (C.3) is

$$\hat{Q}_i(q, \eta) f(\mathbf{k}_i) = \int \frac{d^3k_i}{4\pi} \left[\frac{\Theta_i^+}{\eta - \tau_i - i\delta} - \frac{\Theta_i^-}{\eta - \tau_i + i\delta} \right] f(\mathbf{k}_i), \quad \tau_i = \tau(\mathbf{k}_i, \mathbf{q}), \quad (\text{C.4})$$

defining the integral operator $\hat{Q}_i(q, \eta)$, $i = 1, 2$.

C3: When calculating the CSF C_{1d} , then the Macke function $I(q)$ appears via

$$\int \frac{d\eta}{2\pi i} Q^2(q, \eta) = \frac{2}{(4\pi)^2} I(q), \quad I(q) = \int \frac{d^3k_1 d^3k_2 \Theta_{1,2}^-}{\mathbf{q} \cdot (\mathbf{k}_1 + \mathbf{k}_2 + \mathbf{q})}. \quad (\text{C.5})$$

When dealing with the corresponding exchange term C_{1x} , then by means of contour integration it results

$$\int \frac{d\eta}{2\pi i} \hat{Q}_1(q', \eta) \hat{Q}_2(q', -\eta) v(q') |_{\mathbf{q}' = \mathbf{k}_1 + \mathbf{k}_2 + \mathbf{q}} = \frac{2}{(4\pi)^2} \hat{I}(q) v(|\mathbf{k}_1 + \mathbf{k}_2 + \mathbf{q}|), \quad (\text{C.6})$$

where the integral operator $\hat{I}(q)$ and the exchange term $I_x(q)$ are defined by

$$\hat{I}(q) v(\mathbf{k}_1 + \mathbf{k}_2 + \mathbf{q}) = \int \frac{d^3k_1 d^3k_2 \Theta_{1,2}^-}{\mathbf{q} \cdot (\mathbf{k}_1 + \mathbf{k}_2 + \mathbf{q})} v(|\mathbf{k}_1 + \mathbf{k}_2 + \mathbf{q}|) = I_x(q) v(q). \quad (\text{C.7})$$

$I(q)$ and $I_x(q)$ have the large- q asymptotics

$$\frac{I(q \rightarrow \infty)}{(4\pi/3)^2} = \left(\frac{1}{q^2} + \frac{2}{5} \frac{1}{q^4} + \dots \right), \quad \frac{I_x(q \rightarrow \infty)}{(4\pi/3)^2} = \left(\frac{1}{q^2} + \frac{x}{q^4} + \dots \right). \quad (\text{C.8})$$

Whether the guessed value of $x = 8/5$ [text after (B.7)] is correct, has to be studied. The change of $2/5$ to $8/5$ is a heavy enhancement of the $1/q^4$ -tail, which is plausible in view of the following qualitative arguments. In [9] and [12], the (explicitly not known) function $I_x(q)$ is compared with the explicitly known Macke function $I(q)$. Whereas $I(q)$ starts linearly with q (what causes the Heisenberg divergence), its exchange pendant $I_x(q)$ must start at least with q^2 . Otherwise the integral $\int_0^\infty dq I_x(q)/q^2$ (which is proportional to the

congenially calculated Onsager-et-al energy v_{x2}) would not exist. An estimate shows even $I_x(q \rightarrow 0) \sim q^3$. This flattening in the small- q region together with the "area conservation" $\int_0^\infty dq [I(q) - I_x(q)] = 0$ enforces the mentioned tail enhancement.

C4: Proof of (3.25): In the following the notation

$$\Theta^+(\mathbf{k}, \mathbf{q}) = \Theta(k-1)\Theta(1-|\mathbf{k}+\mathbf{q}|), \quad \Theta^-(\mathbf{k}, \mathbf{q}) = \Theta(1-k)\Theta(|\mathbf{k}+\mathbf{q}|-1) \quad (\text{C.9})$$

is used. (C.4) inserted in (3.25) gives

$$\begin{aligned} X(q, \eta) &= \left[\frac{\Theta(k_1-1)\Theta(1-|\mathbf{k}_1+\mathbf{q}|)}{\eta - \tau(\mathbf{k}_1, \mathbf{q}) - i\delta} - \frac{\Theta(1-k_1)\Theta(|\mathbf{k}_1+\mathbf{q}|-1)}{\eta - \tau(\mathbf{k}_1, \mathbf{q}) + i\delta} \right]_{\mathbf{k}_1 \rightarrow \mathbf{k}-\mathbf{q}} \\ &\quad \cdot \left[\frac{\Theta(k_2-1)\Theta(1-|\mathbf{k}_2+\mathbf{q}|)}{-\eta - \tau(\mathbf{k}_2, \mathbf{q}) - i\delta} - \frac{\Theta(1-k_2)\Theta(|\mathbf{k}_2+\mathbf{q}|-1)}{-\eta - \tau(\mathbf{k}_2, \mathbf{q}) + i\delta} \right]_{\mathbf{k}_2 \rightarrow -\mathbf{k}} \\ &= \left[\frac{\Theta(|\mathbf{k}-\mathbf{q}|-1)\Theta(1-k)}{\eta - \tau(|\mathbf{k}-\mathbf{q}|, \mathbf{q}) - i\delta} - \frac{\Theta(1-|\mathbf{k}-\mathbf{q}|)\Theta(k-1)}{\eta - \tau(|\mathbf{k}-\mathbf{q}|, \mathbf{q}) + i\delta} \right] \\ &\quad \cdot \left[\frac{\Theta(k-1)\Theta(1-|\mathbf{k}-\mathbf{q}|)}{-\eta - \tau(\mathbf{k}, -\mathbf{q}) - i\delta} - \frac{\Theta(1-k)\Theta(|\mathbf{k}-\mathbf{q}|-1)}{-\eta - \tau(\mathbf{k}, -\mathbf{q}) + i\delta} \right]. \end{aligned} \quad (\text{C.10})$$

Only the products "over cross" contribute. With the substitution $\mathbf{q} \rightarrow -\mathbf{q}$ it results

$$X(q, \eta) = \frac{\Theta(k-1)\Theta(1-|\mathbf{k}+\mathbf{q}|)}{[\eta + \tau(\mathbf{k}, \mathbf{q})]^2} + \frac{\Theta(1-k)\Theta(|\mathbf{k}+\mathbf{q}|-1)}{[\eta + \tau(\mathbf{k}, \mathbf{q})]^2} = \frac{\tilde{\Theta}(\mathbf{k}, \mathbf{q})}{[\eta + \tau(\mathbf{k}, \mathbf{q})]^2}. \quad (\text{C.11})$$

To have finally exactly the same expression as in [12] the substitution $\mathbf{k} + \mathbf{q} \rightarrow -\mathbf{k}'$ changes the sign in the dominator, proving thus (3.25).

C5: Proof of (4.1): The diagram of Fig.5a means in detail

$$\begin{aligned} \chi_{1x2}(\mathbf{r}_1|\mathbf{r}'_1, \mathbf{r}_2|\mathbf{r}'_2) &= \frac{1}{4} \int \frac{d^3q_1 d^3q_2}{(4\pi/3)^2} \frac{\omega_{\text{pl}}^4}{q_1^2 q_2^2} \int \frac{d^3k_1 d^3k_2}{(4\pi/3)^2} \\ &\quad \cdot \frac{1}{2} \left\{ e^{i[(\mathbf{k}_2+\mathbf{q}_1+\mathbf{q}_2)\mathbf{r}_{12'}+\mathbf{k}_1\mathbf{r}_{21'}+(\mathbf{q}_1+\mathbf{q}_2)\mathbf{r}_{12}]} \chi_{1x2}(\mathbf{k}_{1,2}, \mathbf{q}_{1,2}) + \text{h.c.} \right\}, \end{aligned} \quad (\text{C.12})$$

where the following abbreviations are used:

$$\chi_{1x2}(\mathbf{k}_{1,2}, \mathbf{q}_{1,2}) = \int \frac{d\omega_1 d\omega_2 d\eta_1 d\eta_2}{(2\pi i)^4} \cdot x_1(\mathbf{k}_1) \cdot x_2(\mathbf{k}_2) \quad \text{with} \quad (\text{C.13})$$

$$\begin{aligned} x_1(\mathbf{k}_1) &= \frac{(k_1 \geq 1)}{\omega_1 - t(\mathbf{k}_1) \pm i\delta} \cdot \frac{(|\mathbf{k}_1 + \mathbf{q}_1| \geq 1)}{\omega_1 + \eta_1 - t(\mathbf{k}_1 + \mathbf{q}_1) \pm i\delta} \cdot \frac{(|\mathbf{k}_1 + \mathbf{q}_1 + \mathbf{q}_2| \geq 1)}{\omega_1 + \eta_1 - \eta_2 - t(\mathbf{k}_1 + \mathbf{q}_1 + \mathbf{q}_2) \pm i\delta}, \\ x_2(\mathbf{k}_2) &= \frac{(k_2 \geq 1)}{\omega_2 - t(\mathbf{k}_2) \pm i\delta} \cdot \frac{(|\mathbf{k}_2 + \mathbf{q}_2| \geq 1)}{\omega_2 - \eta_2 - t(\mathbf{k}_2 + \mathbf{q}_2) \pm i\delta} \cdot \frac{(|\mathbf{k}_2 + \mathbf{q}_1 + \mathbf{q}_2| \geq 1)}{\omega_2 + \eta_1 - \eta_2 - t(\mathbf{k}_2 + \mathbf{q}_1 + \mathbf{q}_2) \pm i\delta}. \end{aligned}$$

For the contribution of the ladder diagram $\chi_{\text{lx}2}$ to the MD $n(k)$, the contraction steps analog (3.21) can be performed with the result

$$\int \frac{d^3 r_{11'}}{2 \cdot 3\pi^2} e^{-i\mathbf{k}\mathbf{r}_{11'}} \int \frac{d^3 r_2}{2 \cdot 3\pi^2} e^{i[(\mathbf{k}_2 + \mathbf{q}_1 + \mathbf{q}_2)\mathbf{r}_{12} + \mathbf{k}_1\mathbf{r}_{21'} + (\mathbf{q}_1 + \mathbf{q}_2)\mathbf{r}_{12}]} = \left(\frac{4\pi}{3}\right)^2 \delta(\mathbf{k}_1 - \mathbf{k})\delta(\mathbf{k}_2 - \mathbf{k}_1)$$

$$\leadsto \hat{\chi}_{\text{lx}2}(k) = \frac{1}{4} \int \frac{d^3 q_1 d^3 q_2}{(4\pi/3)^2} \frac{\omega_{\text{pl}}^4}{q_1^2 q_2^2} \frac{1}{2} \{ \chi_{\text{lx}2}(\mathbf{k}, \mathbf{q}_{1,2}) + \text{c.c.} \} . \quad (\text{C.14})$$

$\chi_{\text{lx}2}(\mathbf{k}, \mathbf{q}_{1,2})$ contains contour integrations in 4 complex frequency planes. Unfortunately, each of these 4 integrals runs over 3 frequency denominators in a difficult way. But by means of a trick (integration variables are substituted) the $\eta_{1,2}$ integrations can be decoupled: $\omega_2 \rightarrow \omega_2 - \eta_1 + \eta_2$. This does not influence $x_1(\mathbf{k})$ (it is only written in reverse order), but it changes $x_2(\mathbf{k})$:

$$x_1(\mathbf{k}_1) = \frac{(|\mathbf{k}_1 + \mathbf{q}_1 + \mathbf{q}_2| \geq 1)}{\omega_1 + \eta_1 - \eta_2 - t(\mathbf{k}_1 + \mathbf{q}_1 + \mathbf{q}_2) \pm i\delta} \cdot \frac{(|\mathbf{k}_1 + \mathbf{q}_1| \geq 1)}{\omega_1 + \eta_1 - t(\mathbf{k}_1 + \mathbf{q}_1) \pm i\delta} \cdot \frac{(k_1 \geq 1)}{\omega_1 - t(\mathbf{k}_1) \pm i\delta} , \quad (\text{C.15})$$

$$x_2(\mathbf{k}) = \frac{k \geq 1}{\omega_2 - \eta_1 + \eta_2 - t(\mathbf{k}) \pm i\delta} \cdot \frac{|\mathbf{k} + \mathbf{q}_2| \geq 1}{\omega_2 - \eta_1 - t(\mathbf{k} + \mathbf{q}_2) \pm i\delta} \cdot \frac{|\mathbf{k} + \mathbf{q}_1 + \mathbf{q}_2| \geq 1}{\omega_2 - t(\mathbf{k} + \mathbf{q}_1 + \mathbf{q}_2) \pm i\delta} . \quad (\text{C.16})$$

Now it is easy to perform the integration over $\eta = \eta_2 - \eta_1$, namely

$$\int \frac{d\eta}{2\pi i} \cdot \frac{(|\mathbf{k} + \mathbf{q}_1 + \mathbf{q}_2| \geq 1)}{\omega_1 - \eta - t(\mathbf{k} + \mathbf{q}_1 + \mathbf{q}_2) \pm i\delta_1} \cdot \frac{(k \geq 1)}{\omega_2 + \eta - t(k) \pm i\delta_2} = \frac{(\mp)(k \geq 1, |\mathbf{k} + \mathbf{q}_1 + \mathbf{q}_2| \geq 1)}{\omega_1 + \omega_2 - t(\mathbf{k}) - t(\mathbf{k} + \mathbf{q}_1 + \mathbf{q}_2) \pm i\delta} . \quad (\text{C.17})$$

Therein those cases do not contribute, where the 2 poles in the complex η -plane are both on the same side of the real axis. Only the combinations $(\pm i\delta_1)$ with $(\mp i\delta_2)$ contribute.

Similarly the η_1 -integration is handled:

$$\int \frac{d\eta_1}{2\pi i} \cdot \frac{(|\mathbf{k} + \mathbf{q}_1| \geq 1)}{\omega_1 + \eta_1 - t(\mathbf{k} + \mathbf{q}_1) \pm i\delta_1} \cdot \frac{(|\mathbf{k} + \mathbf{q}_2| \geq 1)}{\omega_2 - \eta_1 - t(\mathbf{k} + \mathbf{q}_2) \pm i\delta_2} = \frac{(\mp)(|\mathbf{k} + \mathbf{q}_{1,2}| \geq 1)}{\omega_1 + \omega_2 - t(\mathbf{k} + \mathbf{q}_1) - t(\mathbf{k} + \mathbf{q}_2) \pm i\delta} . \quad (\text{C.18})$$

The next step would be the ω_2 -integration. The integrand is a product of the rhs's of (C.17) and (C.18) with the 3rd factor of (C.16):

$$\int \frac{d\omega_2}{2\pi i} \cdot \frac{(\mp)(k \geq 1, |\mathbf{k} + \mathbf{q}_1 + \mathbf{q}_2| \geq 1)}{\omega_1 + \omega_2 - t(\mathbf{k}) - t(\mathbf{k} + \mathbf{q}_1 + \mathbf{q}_2) \pm i\delta} \cdot \frac{(\mp)(k \geq 1, |\mathbf{k} + \mathbf{q}_{1,2}| \geq 1)}{\omega_1 + \omega_2 - t(\mathbf{k}) - t(\mathbf{k} + \mathbf{q}_1) - t(\mathbf{k} + \mathbf{q}_2) \pm i\delta} \cdot \frac{(|\mathbf{k} + \mathbf{q}_1 + \mathbf{q}_2| \geq 1)}{\omega_2 - t(\mathbf{k} + \mathbf{q}_1 + \mathbf{q}_2) \pm i\delta} = \frac{\Theta^\pm(\mathbf{k}, \mathbf{q}_{1,2})}{[\omega_1 - t(\mathbf{k}) + \mathbf{q}_1 \cdot \mathbf{q}_2 \mp i\delta] \mathbf{q}_1 \cdot \mathbf{q}_2} . \quad (\text{C.19})$$

The integration region is defined by the functions $\Theta^\pm(\mathbf{k}, \mathbf{q}_{1,2}) = 1$ for $(k \geq 1, |\mathbf{k} + \mathbf{q}_1 + \mathbf{q}_2| \geq 1, |\mathbf{k} + \mathbf{q}_{1,2}| \leq 1)$ and 0 otherwise. The identity

$$t(\mathbf{k}) + t(\mathbf{k} + \mathbf{q}_1 + \mathbf{q}_2) - t(\mathbf{k} + \mathbf{q}_1) - t(\mathbf{k} + \mathbf{q}_2) = \mathbf{q}_1 \cdot \mathbf{q}_2 \quad (\text{C.20})$$

is used. The remaining ω_1 -integration finally yields

$$\chi_{1 \times 2}(\mathbf{k}, \mathbf{q}_{1,2}) = \int \frac{d\omega_1}{2\pi i} \frac{\Theta^\pm(\mathbf{k}, \mathbf{q}_{1,2})}{[\omega_1 - t(\mathbf{k}) \pm i\delta][\omega_1 - t(\mathbf{k}) + \mathbf{q}_1 \cdot \mathbf{q}_2 \mp i\delta]} = \frac{\Theta(\mathbf{k}, \mathbf{q}_{1,2})}{(\mathbf{q}_1 \cdot \mathbf{q}_2)^2} \quad (\text{C.21})$$

where $\Theta = \Theta^+ + \Theta^-$. (C.21) inserted in (C.14) gives (4.1), qed .

Appendix D: Correlation parameters

Here is a list of characteristic correlation parameters as functions of r_s , vanishing for $r_s \rightarrow 0$:

$N = \int_0^\infty d(k^3) [n(k) - n_0(k)]$ is the normalization of the MD-correlation tails.

$c = \int_0^\infty d(k^3) n(k)[1 - n(k)] = N - \int_0^\infty d(k^3) [n(k) - n_0(k)]^2$ is the Löwdin parameter.

$1 - z_F$ is the reduced discontinuity jump of $n(k)$ at the Fermi surface $|\mathbf{k}| = 1$.

$s = - \int_0^\infty d(k^3) [n(k) \ln n(k) + (1 - n(k)) \ln(1 - n(k))]$ is the particle-hole symmetric correlation entropy, see Eq.(22) in [22].

$c_1 = h_a(0)$ with $1 - h_a(0) = g_a(0)$ being the on-top value of the Coulomb hole,

c_1 simultaneously determines the large- q asymptotics of $C_{d,x}(q)$ and $n(k)$,

c_2, c'_2 determine the higher-order large- q asymptotics of $C_{d,x}(q)$,

$c_3 = h_p''(0)$ and t determine the on-top curvature of the Fermi hole $g_p''(0) = \frac{4}{3}t - h_p''(0)$,

$c_{4,5}$ determine the small- q behavior of $S(q)$ beyond the plasmon-SR term $q^2/(2\omega_{pl})$,

c_6 influences the jump discontinuity $\Delta S''(2)$.

All these parameters may serve as measures of the correlation strength. They vanish for $r_s \rightarrow 0$ with terms $\sim r_s, r_s^2 \ln r_s$ or $r_s^{3/2}$. From a diagrammatical point of view all the quantities characterizing $n(k)$ or derived from it, should start with r_s^2 . The reason: the diagrams for $n(k)$ start with $n_2(k)$, the 1st-order term $n_1(k)$ (Fig. 4c) is zero - in agreement with the vanishing 1st-order kinetic energy $t_1 = 0$, what follows from the virial theorem (1.1). But there are starting dependencies as $N = O(r_s^{3/2})$ cf (3.46) in [12]. This peculiar behavior is an example for how higher-order partial summations may create lower-order terms. It is a peculiarity of the Coulomb repulsion. $N \sim r_s^{3/2}$ results from that k -region $|k-1| \ll q_c$, where the RPA reconstruction takes place. A characteristic non-analyticity is also the behavior of

$n(k)$ at the Fermi surface $|\mathbf{k}| = 1$, namely $\sim (k - 1) \ln |k - 1|$.

- [1] M.P. Tosi in: N.H. March (Ed.), *Electron Correlation in the Solid State*, Imperial College Press, 1999, p. 1. - G. Giuliani and G. Vignale, *Quantum Theory of the Electron Liquid*, Cambridge University Press, Cambridge, 2005.
- [2] There is a non-vanishing probability of finding 0, 2, 3, ... electrons in such a Wigner sphere. Such particle number fluctuations in fragments have been studied by P. Ziesche, J. Tao, M. Seidl, and J.P. Perdew, *Int. J. Quantum Chem.* **77**, 819 (2000) with the conclusion ‘correlation suppresses fluctuations’, cf also P. Fulde, *Electron Correlations in Molecules and Solids*, 3rd ed., Springer, Berlin, 1995, p. 157.
- [3] The Coulomb repulsion takes the form $\alpha r_s/r$, if lengths and energies are measured in units of k_F^{-1} and k_F^2 , respectively. This shows, that r_s is not only a density parameter [2], but also measures the interaction strength or coupling constant. The FT of $\alpha r_s/r$ is $4\pi\alpha r_s/q^2 = \pi^2(q_c^2/q^2)$ with q measured in units of k_F and $q_c^2 = 4\alpha r_s/\pi$. - Notice that $\tilde{e} = k_F^2 e = e/(\alpha r_s)^2$ gives the energy in a.u., e.g. the energy in zeroth order and the lowest-order exchange energy are $\tilde{e}_0 = 3/(10 \alpha^2 r_s^2)$ and $\tilde{e}_x = -3/(4\pi\alpha r_s)$, respectively.
- [4] J. Cioslowski, P. Ziesche, and K. Pernal, *Phys. Rev. B* **63**, 205105 (2001); *J. Chem. Phys.* **115**, 8725 (2001).
- [5] P. Ziesche, *Int. J. Quantum Chem.* **90**, 342 (2002). The last sentence of the Abstract has to be deleted.
- [6] P. Ziesche and J. Cioslowski, *Physica A* **356**, 598 (2005). - Here it is shown, which peculiarities of $n(k)$ and $S(q)$ caused by RPA lead to the logarithmic non-analyticity of the high-density correlation energy $e_{\text{corr}} \sim r_s^2 \ln r_s$. - In Eq. (27) the correct prefactor is $2\alpha r_s/(5\pi)$.
- [7] R. Diez Muiño, I. Nagy, and P.M. Echenique, *Phys. Rev. B* **72**, 075117 (2005).
- [8] J. Cioslowski and P. Ziesche, *Phys. Rev. B* **75**, 085103 (2007). Here the self-energy $\Sigma(1, 1/2)$ is investigated.
- [9] P. Ziesche, *phys. stat. sol. (b)* **244**, 2022 (2007); the relation $\mu - \mu_0 = \Sigma(1, \mu)$ has been studied for $r_s \rightarrow 0$. - In Appendix C the Macke function $I(q)$ is explicitly given. The notation $I(q)$ is related to the notation used in [29] as $\Delta S(q/2)_D = -3/(8\pi^2)(q_c/q)^2 I(q)$ and in [6] as $K(q) = 3/(8\pi^2 q^2) I(q)$.

- [10] P. Ziesche, Ann. Physik (Leipzig) **16**(1), 45 (2007). Here it has been shown $\Sigma_{2x}(1, 1/2) = e_{2x}$.
- [11] M.L. Glasser and G. Lamb, J. Phys. A **40**, 1215 (2007).
- [12] P. Ziesche, Ann. Phys. (Berlin) **522**(10), 739 (2010). - In the 2nd line of Eq. (C.19) there is a prefactor q^2 missing. Read the last line on p. 762 as "respectively. One may guess, that $I_x(q)$ starts with $\sim q^3$." .
- [13] W. Heisenberg, Z. Naturf. **2a**, 185 (1947).
- [14] W. Macke, Z. Naturf. **5a**, 192 (1950). - Another access with the same result is due to D. Bohm and D. Pines, Phys. Rev. **92**, 609 (1953) and D. Pines, Phys. Rev. **92**, 626 (1953).
- [15] M. Gell-Mann and K. Brueckner, Phys. Rev. **106**, 364 (1957).
- [16] N.H. March, Phys. Rev. **110**, 604 (1958). - Note that the "Hellmann-Feynman theorem" had been formulated first by P. Güttinger, Z. Phys. **73**, 169 (1932); later it was to be found in H. Hellmann, Einführung in die Quantenchemie (Deuticke, Leipzig, 1937), pp. 61 and 285 as well as in R.P. Feynman, Ph.D. Thesis, MIT, 1939; Phys. Rev. **56**, 340 (1939).
- [17] D. Pines and P. Nozières, The Theory of Electron Liquids, Vol. I (Benjamin, New York, 1966).
- [18] From the f -SR or Thomas-Reich-Kuhn SR of the dynamic SF $S(q, \omega)$ follows the plasmon SR $S(q \ll q_c) = q^2/(2\omega_{pl}) + \dots$ of the static SF $S(q)$.
- [19] E. Daniel and S.H. Vosko, Phys. Rev. **120**, 2041 (1960).
- [20] I.O. Kulik, Zh. Éksp. Teor. Fiz. **40**, 1343 (1961) [Sov. Phys. JETP **13**, 946 (1961)].
- [21] P. Ziesche, phys.stat.sol. (b) **232**, 231 (2002).
- [22] P. Gori-Giorgi and P. Ziesche, Phys. Rev. B **66**, 235116 (2002). - An *analytical* expression for $n(k)$ in the range $r_s = 1, \dots, 10$ is carefully fitted to the well-known kinetic energy $t(r_s)$. - For the momentum distributions of the spin-polarized electron gas see [23].
- [23] P. Ziesche and F. Tasnádi, Ann. Physik (Leipzig) **13**, 124 (2004), Erratum **13**, 623 (2004), Sec.4, Fig.2. - Besides in Sec.5 it is also presented the spin-structure of the spin-polarized HEG.
- [24] M. Holzmann, B. Bernu, C. Pierleoni, J. McMinis, D.M. Ceperley, V. Olevano, and L.D. Site, Phys. Rev. Lett. **107**, 110402 (2011) with Monte Carlo calculations for $n(k)$.
- [25] P. Ziesche, Thesis, TH Dresden, 1963; Ann. Phys. (Leipzig) **21**, 80 (1968).
- [26] I.A. Nechaev and E.V. Chulkov, Phys. Rev. B **73**, 165112 (2006).
- [27] A.J. Glick and R.A. Ferrell, Ann. Phys. **11**, 359 (1960).
- [28] D.J. Geldart, Can. J. Phys. **45**, 3139 (1967).

- [29] J.C. Kimball, Phys. Rev. B **14**, 2371 (1976).
- [30] D.M. Ceperley and B.J. Alder, Phys. Rev. Lett. **45**, 566 (1980), with Monte Carlo calculations for $g(r)$. Other papers are based eg on the dielectric function $\varepsilon(k, \omega)$ and local field corrections.
- [31] J.C. Kimball, Phys. Rev. A **7**, 1648 (1973).
- [32] A.K. Rajagopal, J.C. Kimball, M. Banerjee, Phys. Rev. B **18**, 2339 (1978).
- [33] D.J.W. Geldart, A. Houghton, S.H. Vosko, Can. J. Phys. **42**, 1938 (1964).
- [34] P. Ziesche and F. Tasnádi, Ann. Phys. (Leipzig) **13**, 232 (2004); Erratum **13**, 624 (2004).
- [35] N. Iwamoto, Phys. Rev. A **33**, 1940 (1986), Eq. (4.2).
- [36] P. Gori-Giorgi, F. Sacchetti, G.B. Bachelet, Physica A **280**, 199 (2000), Table on p. 201; Phys. Rev. B **61**, 7353 (2000); Phys. Rev. B **66**, 159901(E)(2002).
- [37] L. Zecca, P. Gori-Giorgi, S. Moroni, and G.B. Bachelet, Phys. Rev. B **70**, 205127 (2004).
- [38] L. Onsager, L. Mittag, and M. J. Stephen, Ann. Physik (Leipzig) **18**, 71 (1966). Here the exchange integral of the 3-dimensional HEG has been evaluated *analytically*. This rather herculean work was generalized and extended to the d -dimensional electron gas by M.L. Glasser [39].
- [39] M.L. Glasser, J. Comp. Appl. Math. **10**, 293 (1984).
- [40] P. Ziesche, Commun. Math. Phys. **5**, 301 (1967).
- [41] P. Ziesche, in: J. Cioslowski (Ed.), *Many-Electron Densities and Reduced Density Matrices*, Kluwer Academic/Plenum Publishers, New York, 2000, p. 33.
- [42] P. Ziesche, Lecture Series on Computer and Computational Sciences **7b**, 1051, (2006).
- [43] Z. Qian, Phys. Rev. B **73**, 035106 (2006).
- [44] J. Cioslowski and P. Ziesche, Phys. Rev. B **71**, 125105 (2005); Phys. Rev. B **72**, 239901(E)(2005).
- [45] J.C. Kimball, J. Phys. A **8**, 1513 (1975).
- [46] H. Yasuhara and Y. Kawazoe, Physica **85A**, 416 (1976).
- [47] V.A. Rassolov, J.A. Pople, and M.A. Ratner, Phys. Rev. B **62**, 2232 (2000).
- [48] A.W. Overhauser, Can. J. Phys. **73**, 683 (1995). Succeeding papers are [49–53].
- [49] P. Gori-Giorgi and J.P. Perdew, Phys. Rev. B **64**, 155102 (2001): Extended Overhauser model. P. Gori-Giorgi and A. Savin, Phys. Rev. A **73**, 032506 (2006): Electron-electron coalescence and short- and long-range correlation.
- [50] M. Corona, P. Gori-Giorgi, and J.P. Perdew, Phys. Rev. B **69**, 045108 (2004).

- [51] R. Asgari, M. Cardenas, M. Polini, B. Davoudi, and M.P. Tosi, cond-mat/0408293.
- [52] P. Ziesche, Phys. Rev. B **67**, 233102 (2003).
- [53] P. Ziesche, phys. stat. sol. (b) **241**, 3544 (2004): I; (b) **242**, 2051 (2005): II. - It is shown, that the Kimball-Overhauser geminals do not satisfy the plasmon SR.
- [54] H. Yasuhara, Solid State Commun. **11**, 1481 (1972); Physica **78**, 420 (1974); J.M. Herbert, Phys. Rev. A **66**, 052502 (2002); R. Asgari, M. Polini, B. Davoudi, and M.P. Tosi, Solid State Commun. **125**, 139 (2003).
- [55] L. Kong and E.F. Valeev, J. Chem. Phys. **134**, 214109 (2011).
- [56] D.R. Alcoba, R.C. Bochicchio, L. Lain, and A. Torre, J. Chem. Phys. **133**, 144104 (2010).
- [57] K.R. Shamasundar, J. Chem. Phys. **131**, 174109 (2009).
- [58] S.D. Hamieh and H. Zaraket, Eur. Phys. J. D **55**, 229 (2009).
- [59] M. Nooijen, M. Wladyslawski, and A. Hazra, J. Chem. Phys. **118**, 4832 (2003).
- [60] D.A. Mazziotti (Ed.), *Reduced Density Matrices: With Applications to Many-Electron Atoms and Molecules*, Wiley-Blackwell, Hoboken, 2007; T. Juhász and D.A. Mazziotti, J. Chem. Phys. **125**, 174105 (2006).
- [61] J.M. Herbert, Int. J. Quantum Chem. **107**, 703 (2007).
- [62] J.M. Herbert, "Reconstructive Approaches to One- and Two-Electron Density Matrix Theory", Dissertation, Uni of Wisconsin-Madison, 2003, p. 88.
- [63] J.E. Harriman, Phys. Rev. A **65**, 052507 (2002).
- [64] W. Kutzelnigg and D. Mukherjee, J. Chem Phys. **110**, 2800 (1999); Chem. Phys. Lett. **317**, 567 (2000).
- [65] W.H. Young and N.H. March, Proc. Roy. Soc. A **256**, 62 (1960).
- [66] M. Nakata, B.J. Braams, K. Fujisawa, M. Fukuda, J.K. Percus, M. Yamashita, and Zh. Zhao, J. Chem. Phys. **128**, 164113 (2008).
- [67] J.Sun, J.P. Perdew, and M. Seidl, Phys. Rev. B **81**, 085123 (2010). The correlation energy is interpolated between high- and low-density limits.
- [68] P.-F. Loos and P.W. Gill, Phys. Rev. B **84**, 033103 (2011). Here, the spin-polarized HEG at high-density is treated.
- [69] The GS-energy e is also a functional of $t(\mathbf{k})$ and $v(\mathbf{q})$ with $\delta e/\delta t(\mathbf{k}) \sim n(k)$ [19] and $\delta e/\delta v(\mathbf{q}) \sim S(q) - 1$ [29, 70].
- [70] H. Yasuhara, Physica **78**, 420 (1974).

Figures

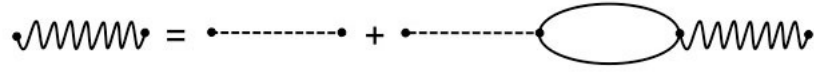


FIG. 1: Feynman diagrams for the Coulomb repulsion in RPA with the partial summation (or screening replacement) $v(q) \rightarrow v(q, \eta)$, q = momentum transfer, η = energy/frequency, dashed line = bare interaction $v(q) = q_c^2/q^2$, closed loop = particle-hole propagator $Q(q, \eta)$ of (C.3), wavy line = effectively screened interaction $v(q, \eta) = v(q)/[1 + v(q)Q(q, \eta)]$.

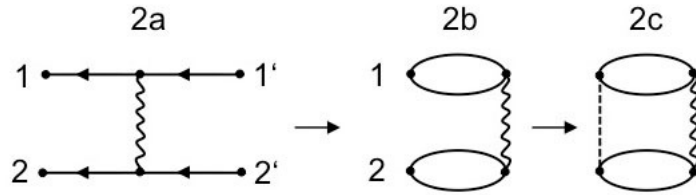


FIG. 2: 2a = lowest-order renormalized cumulant 2-matrix χ_{dr} , 2b = non-divergent cumulant PD h_{dr} or cumulant SF C_{dr} (Kimball) [31], 2c = non-divergent interaction energy v_{dr} (Macke, Gell-Mann/Brueckner) [14, 15].

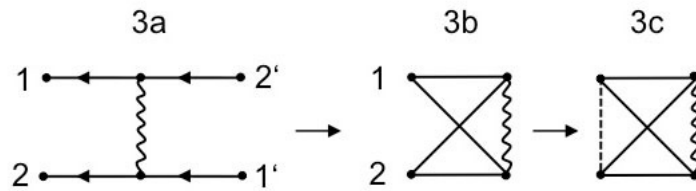


FIG. 3: The RPA exchange terms corresponding to Fig.2 with 3a = χ_{xr} (following from 2a = χ_{dr} through the exchange replacement $1' \leftrightarrow 2'$), 3b = h_{xr} or C_{xr} (non-divergent), and 3c = v_{xr} . As shown by Onsager et al. [38], already v_{x2} does not diverge (needs no RPA renormalization).

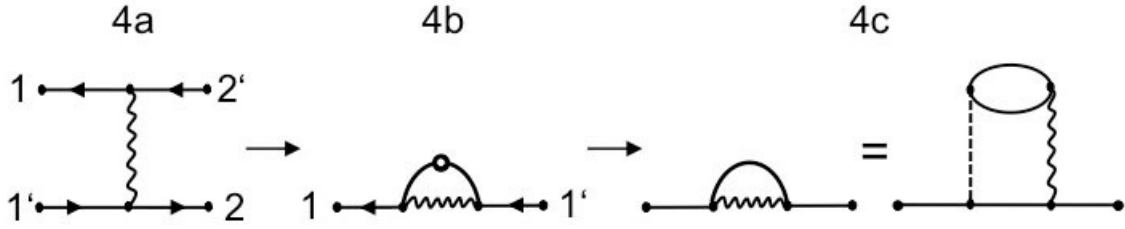


FIG. 4: How the 2-body diagram $4a = 3a = \chi_{\text{xr}}$ transforms to the 1-body diagram 4b through the contraction [with $2'=2$ and $\int d2$, see (2.25)], marked by a small circle and finally to the non-divergent RPA-diagram $n_r(k)$ of Fig.4c (Daniel/Vosko and Kulik) [19, 20]. The 1st-order term is zero (analog to the 1st-order kinetic energy $t_1 = 0$).

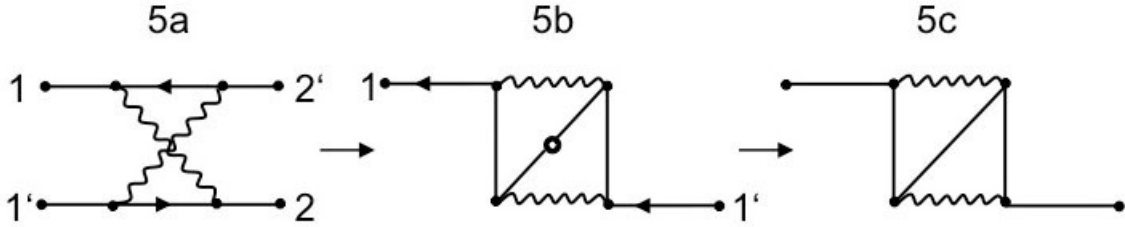


FIG. 5: How the 2-body ladder diagram 5a in its exchange version χ_{lxr} transforms to the 1-body diagram 5b through the contraction (2.25) and finally to the diagram $n_x(k)$ of Fig.5c. In Sec.IV and App.C5 the RPA screening is neglected for simplicity corresponding to the replacement $r \rightarrow 2$ or $v(q, \eta) \rightarrow v(q)$.

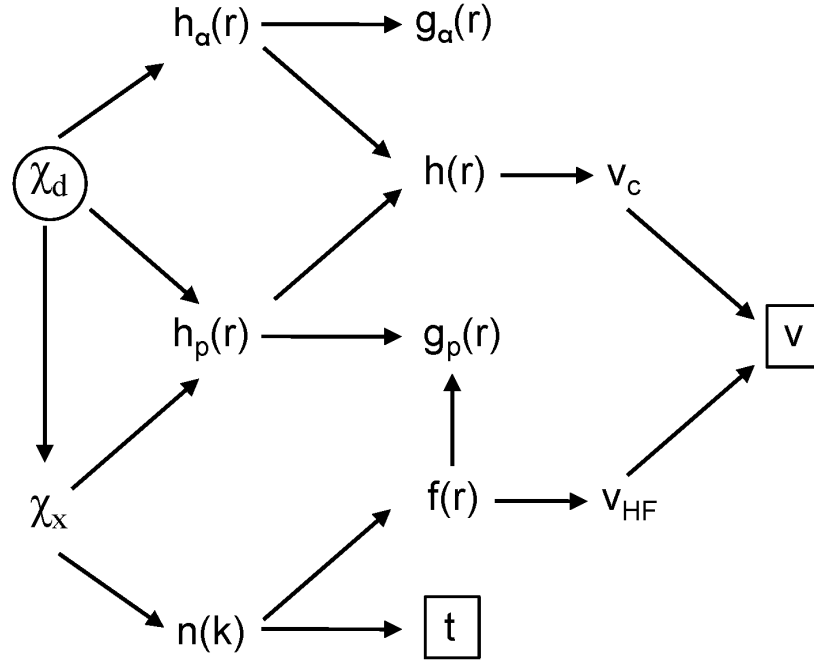


FIG. 6: Flow charts showing the way from the starting point $\chi_d =$ direct cumulant 2-matrix through its exchange pendant χ_x and the cumulant PD $h(r)$ to the final results $n(k)$ and $g(r)$, from which follow (i) $f(r) =$ 1-matrix, $t =$ kinetic energy, $c =$ Löwdin parameter and (ii) $v =$ interaction energy, respectively. "a"=spin-antiparallel, "p"=spin-parallel. From FT arises a similar scheme for the structure factor $S(q)$, the cumulant structure factor $C(q)$, and the HF term $F(q)$ [$\leftrightarrow g(r)$, $h(r)$, and $f^2(r)$, respectively]. Note that $g(r) = \frac{1}{2}[g_a + g_p(r)]$ and $e = t + v$.

Table 1: The behavior of the cumulant structure factors (CSFs) vs. q . Note $C_a = C_d$ and $C_p = C_d - C_x$. The index "a" means spin-antiparallel, "p" means spin-parallel, d = direct (2-line) diagram, x = corresponding exchange (1-line) diagram. The total CSF is $C = C_a + C_p$. For the Löwdin parameter c see (2.13), for c_1 see (B.4). The cubic term of $C_x(q \ll q_c)$ is chosen such that the total SF S has the correct small- q behavior $q^2/(2\omega_{\text{pl}}) + O(q^4)$ [35].

CSF	$q \ll q_c$	$q \rightarrow \infty$	$\int_0^\infty d(q^3) \dots$
$C_d(q)$	$z_{\text{F}}^2 \left(\frac{3q}{8} - \frac{q^3}{32} \right) - \frac{q^2}{4\omega_{\text{pl}}} + \left[s_4 \left(\frac{q}{\omega_{\text{pl}}} \right)^4 + s_5 \left(\frac{q}{\omega_{\text{pl}}} \right)^5 + \dots \right] \omega_{\text{pl}} + \dots$	$\left(\frac{1-c_1}{q^4} + \frac{2/5+c_2}{q^6} + \dots \right) \omega_{\text{pl}}^2 + \dots$	c_1
$C_x(q)$	$-c + \left[s_4' \left(\frac{q}{\omega_{\text{pl}}} \right)^4 + s_5' \left(\frac{q}{\omega_{\text{pl}}} \right)^5 + \dots \right] \omega_{\text{pl}} + \dots$	$\left(\frac{1-c_1}{q^4} + \frac{8/5+c_2'}{q^6} + \dots \right) \omega_{\text{pl}}^2 + \dots$	c_1
$C_a(q)$	$z_{\text{F}}^2 \left(\frac{3q}{8} - \frac{q^3}{32} \right) - \frac{q^2}{4\omega_{\text{pl}}} + \left[s_4 \left(\frac{q}{\omega_{\text{pl}}} \right)^4 + s_5 \left(\frac{q}{\omega_{\text{pl}}} \right)^5 + \dots \right] \omega_{\text{pl}} + \dots$	$\left(\frac{1-c_1}{q^4} + \frac{2/5+c_2}{q^6} + \dots \right) \omega_{\text{pl}}^2 + \dots$	c_1
$C_p(q)$	$c + z_{\text{F}}^2 \left(\frac{3q}{8} - \frac{q^3}{32} \right) - \frac{q^2}{4\omega_{\text{pl}}} + \left[s_4'' \left(\frac{q}{\omega_{\text{pl}}} \right)^4 + s_5'' \left(\frac{q}{\omega_{\text{pl}}} \right)^5 + \dots \right] \omega_{\text{pl}} + \dots$	$\left(\frac{-6/5+c_2-c_2'}{q^6} + \dots \right) \omega_{\text{pl}}^2 + \dots$	0
$C(q)$	$c + z_{\text{F}}^2 \left(\frac{3q}{4} - \frac{q^3}{16} \right) - \frac{q^2}{2\omega_{\text{pl}}} + \left[s_4''' \left(\frac{q}{\omega_{\text{pl}}} \right)^4 + s_5''' \left(\frac{q}{\omega_{\text{pl}}} \right)^5 + \dots \right] \omega_{\text{pl}} + \dots$	$\left(\frac{1-c_1}{q^4} + \frac{-4/5+2c_2-c_2'}{q^6} + \dots \right) \omega_{\text{pl}}^2 + \dots$	c_1

Table 2: The behavior of the structure factors (SFs) vs. the momentum transfer q . Note $S_a = -C_a$ and $S_p = 1 - \frac{1}{2}F - C_p$. The total SF is $S = S_p + S_a = 1 - \frac{1}{2}F - C$, the magnetic SF is $M = S_p - S_a$.

SF	$q \ll q_c$	$q \rightarrow \infty$	normalization
$\frac{1}{2}F(q)$	$1 - c - z_F^2 \left(\frac{3q}{4} - \frac{q^3}{16} \right) + \dots$	$\frac{1-c_1}{8} \frac{\omega_{\text{pl}}^4}{q^8} + \dots$	$\int_0^\infty d(q^3) \frac{1}{2}F(q) = 1$
$S_a(q)$	$-z_F^2 \left(\frac{3q}{8} - \frac{q^3}{32} \right) + \frac{q^2}{4\omega_{\text{pl}}} - \left[s_4 \left(\frac{q}{\omega_{\text{pl}}} \right)^4 + s_5 \left(\frac{q}{\omega_{\text{pl}}} \right)^5 + \dots \right] \omega_{\text{pl}} + \dots$	$-\left(\frac{1-c_1}{q^4} + \frac{2/5+c_2}{q^6} + \dots \right) \omega_{\text{pl}}^2 + \dots$	$\int_0^\infty d(q^3) S_a(q) = -c_1$
$S_p(q)$	$z_F^2 \left(\frac{3q}{8} - \frac{q^3}{32} \right) + \frac{q^2}{4\omega_{\text{pl}}} - \left[s_4'' \left(\frac{q}{\omega_{\text{pl}}} \right)^4 + s_5'' \left(\frac{q}{\omega_{\text{pl}}} \right)^5 + \dots \right] \omega_{\text{pl}} + \dots$	$1 - \left(\frac{-6/5+c_2-c'_2}{q^6} + \dots \right) \omega_{\text{pl}}^2 + \dots$	$\int_0^\infty d(q^3) [1 - S_p(q)] = 1$
$S(q)$	$\frac{q^2}{2\omega_{\text{pl}}} - \frac{1}{2} \left[\left(\frac{1}{3^2} + C_4 \right) \left(\frac{q}{\omega_{\text{pl}}} \right)^4 - \left(\frac{2^2}{3^{3 \cdot 5}} + C_5 \right) \left(\frac{q}{\omega_{\text{pl}}} \right)^5 + \dots \right] \omega_{\text{pl}} + \dots$	$1 - \left(\frac{1-c_1}{q^4} + \frac{-4/5+2c_2-c'_2}{q^6} + \dots \right) \omega_{\text{pl}}^2 + \dots$	$\int_0^\infty d(q^3) [1 - S(q)] = 1 + c_1$
$M(q)$	$z_F^2 \left(\frac{3q}{4} - \frac{q^3}{16} \right) + \left[O \left(\frac{q}{\omega_{\text{pl}}} \right)^4 + \dots \right] \omega_{\text{pl}} + \dots$	$1 + \left(\frac{1-c_1}{q^4} + O \left(\frac{1}{q^6} \right) + \dots \right) \omega_{\text{pl}}^2 + \dots$	$\int_0^\infty d(q^3) [1 - M(q)] = 1 - c_1$